conditions vary with time, a new operating point has to be found for every timestep throughout a simulation. The first guess within a timestep is always chosen to be the voltage at the previously calculated operating point, except for the very first timestep of the simulation, at which incident radiation occurs. At this particular point, nothing is known about where the operating point is going to be. The voltage at maximum power point is a good guess, since in the ideal case a load should be designed to operate close to that point.

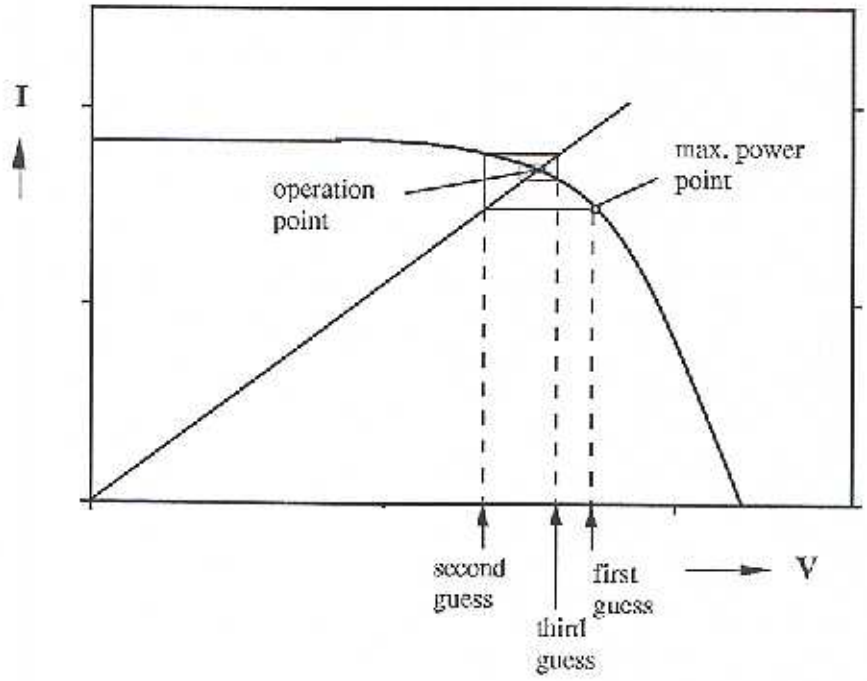

Figure 2.10 Convergence by successive substitution

The problem involved in using the current as input to the PV array component is best explained by looking at the PV cell I-V curve in Figure 2.10. At low voltages, the cell acts almost like a constant current source. Guessing a current in that region would not result in an unambiguous voltage value, therefore it is not possible to obtain a solution.

Another issue which has to be discussed is the question of whether the proposed method converges under all conditions. Convergence depends on the slope of the load I-V curve relative to the slope of the PV cell I-V curve. An example of divergence is shown in Figure 2.11. For this reason a numerical convergence promoting method is integrated in the PV array component.

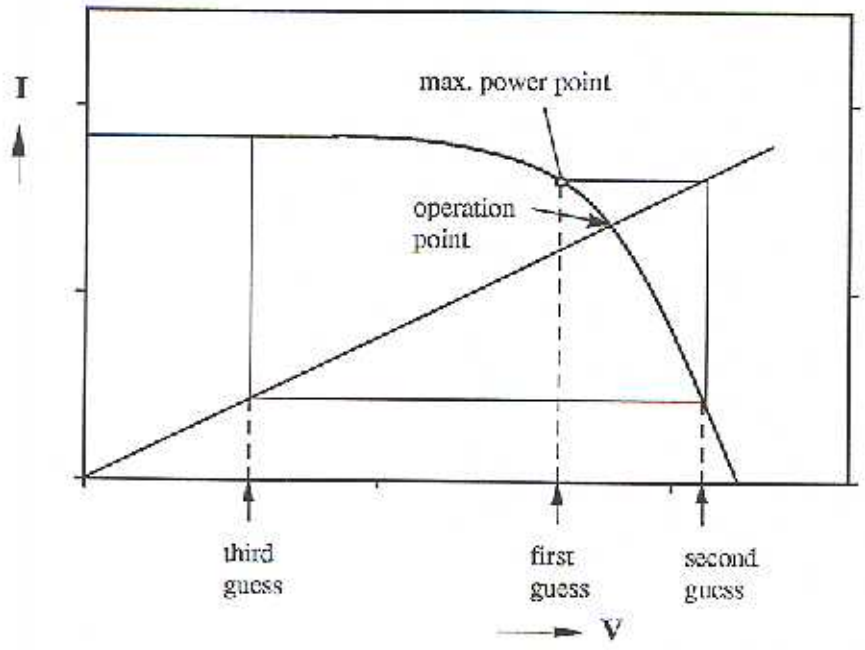

Figure 2.11 Divergence by successive substitution

The convergence promoter consists basically of a bisection type search method. A lower and an upper limit for the voltage is set and a new voltage is found by cutting the interval in half. This voltage is then used to compute the cell current, which is then shifted to the load component. Depending upon the circumstances, the interval limits are set differently. As mentioned earlier, the first guess is the voltage at the previously

calculated operating point. The returning voltage is tracked for the next two iterations and compared to the first guess voltage. Thus it is possible to tell where the load I-V curve is located relative to the first guess voltage and the limits can be set appropriately. Hence the actual interval cutting procedure is first invoked at the beginning of the third iteration. An exception for that is, if the returning voltage after the first iteration is already out of the PV cell voltage range (i.e. is greater than the open circuit voltage). In this case the open circuit voltage is used as the upper limit and the lower limit is determined by the first guess voltage, and the *Bisection method* can be used right away. Figure 2.12 illustrates how the procedure works for a situation where the successive substitution method, performed by *TRNSYS*, would diverge. Only the first couple of iterations are shown.

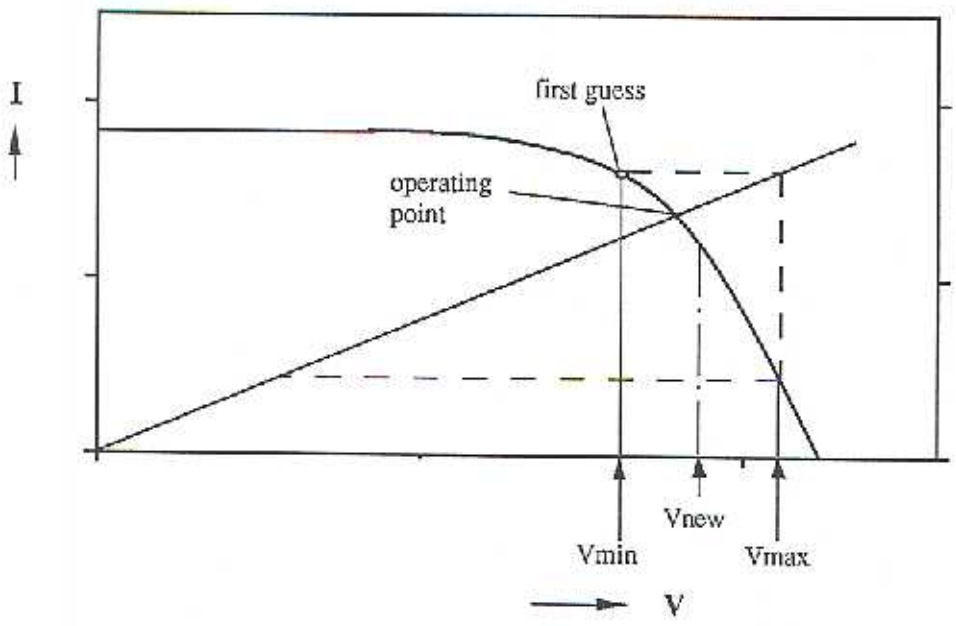

Figure 2.12 Illustration of convergence procedure

In the special case when the I-V curve intersects the PV cell I-V curve in the region of constant current, the *TRNSYS* method converges already after two iterations, and the convergence promoter is not invoked. Many different situations are possible and the convergence promotion algorithm takes care of all them.

The fourth input variable, Flag, is a signal to turn the convergence promoter on or off. The convergence promoter has to be turned off when simulating a system with battery storage. This will be explained more detailed in Chapter 6. Simulating direct coupled systems requires the use of the convergence promoter. If Flag is equal to one, the convergence promoter is on, otherwise it is off.

Most of the outputs are self explanatory. The fifth output, Util, is the utilization of the PV array expressed as the ratio of the power at the operation point to the maximum power:

$$\text{Util} = \frac{P}{P_{max}}$$

The Fortran code for the component program is listed in Appendix A.

Chapter 3

LOAD CHARACTERISTICS

The behavior of any electrical load can be characterized by its I-V curve. The I-V curve shows all the possible points where the load may be operated. The actual operating point, e.g. for a direct coupled PV system is the intersection of the PV array and the load I-V curve. In this chapter several types of loads are investigated. Mathematical relations describing the load I-V curves are derived and *TRNSYS* components are formulated.

In the first section, an ohmic resistance type of load is discussed. The following sections cover inductive loads. In particular, a series DC motor and a separately excited permanent magnet DC motor are investigated. As mechanical loads driven by the DC motors, a centrifugal fan and a centrifugal pump are chosen.

A preceding comment has to be made about the selected inputs and outputs of the developed *TRNSYS* components. As mentioned in Section 2.6, the operating point of a system is found via an iterative process between the system components. The information transferred between the components is the voltage and the current. Regarding a direct coupled system, the information shifted from the PV array component to the load component is the current for reasons explained in Section 2.6. In a system including battery storage, the operating voltage range is mainly determined by the terminal voltage of the battery if it is continously connected. Although the

battery voltage varies with the battery current and the state of charge of the battery, the change in battery voltage is relatively small. This fact is used to determine the operating voltage of a system with battery storage by shifting the voltage of the battery component to the load components. This will be explained in detail in Chapters four and five. That means that all load components have current and voltage as input. The load components must have the capability to compute, depending on the significant input, the respective quantity which is then subject of the iterative process in finding the operating point. An additional input serves as a control signal to determine which of the inputs, current or voltage, is significant.

3.1 RESISTANCE

Lighting and heating are representative applications for resistive loads. The I-V curve of a resistance is described by *Ohm's* law:

$$V = I R \tag{3.1}$$

where R is the resistance.

As discussed in Chapter 2.6, the I-V curve is a straight line through the origin with the slope 1/R as shown in Figure 2.8.

3.2 TRNSYS COMPONENT OF A RESISTANCE

The construction of the information flow diagram for a resistance, as illustrated in Figure 3.1, is very simple. The inputs are the current, the voltage and a signal called Mode. Mode determines whether current or voltage is the significant input. When running direct coupled systems, Mode has to be set equal to one. This fixes the current as input and the output voltage is computed corresponding to equation (3.1). In a system where the voltage serves as input to the load, Mode has to be zero and the calculations are in reverse order. The only parameter of the component is the resistance value.

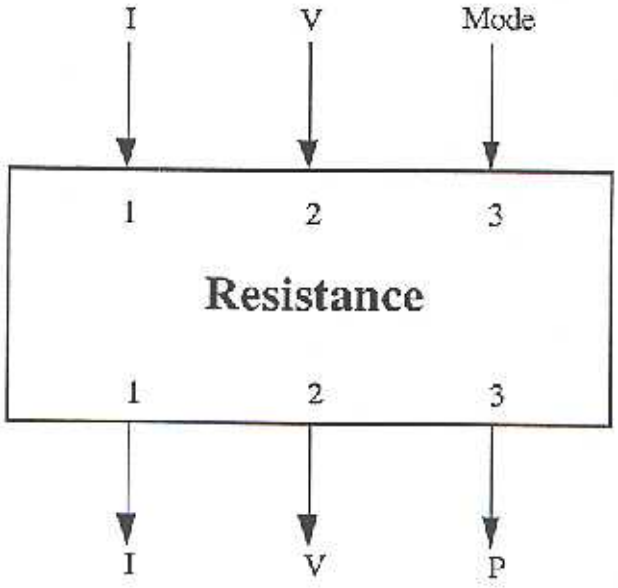

Figure 3.1 Information flow diagram of the resistance component

The parameter of the component is:

R = resistance [ohms]

3.3 MOTOR LOADS

Motor loads are composed of two components: an electrical motor and a mechanical subload driven by the motor. Of interest are the speed-torque characteristics of both components. Once the speed-torque behavior of the two components are known, the operating conditions of the load subsystem can be found. The overall goal is to determine the operating point of the entire PV system. This is best examined in the electrical I-V plane, looking at the PV array and load I-V curves. The load I-V curve of a motor load is obtained by transposing the possible operating points of the load subsystem from the mechanical speed-torque plane into the I-V plane applying fundamental equations presented in this section. The emphasis of this chapter is on finding the load I-V curves. The behavior of the entire PV system is discussed in Chapter 5.

Regarding the DC-motors applied to a centrifugal fan load, similar studies have been conducted by Appelbaum [7,8,9,10,11], Roger [12] and Townsend [3]. Braunstein et al. [13] and Hsiao [14] investigated motor-water pump loads. The following assumptions apply to the modelling of the DC-motors [15]:

- The magnetic flux is linearly dependent on field current. This is the case when the iron core in the field inductor is not magnetized beyond its saturation point.
- Hysteresis effects are neglected.
- The armature and field inductances are constant. This is based on uniform windings geometry and negligible temperature effects.
- Armature reaction is negligible. This assumes the motor operates at or

below its rated current, and is also a consequence of the first assumption.

- The brush voltage drop is neglected.
- A linear function is assumed to describe the total loss torque of the motors: $T_{loss} = C_{stat} + C_{visc}\,\omega$ where C_{stat} is a static friction, C_{visc} is a viscous friction and ω is the angular velocity. Losses are caused by bearing friction, brush friction, friction with air (windage), hysteresis and eddy current losses.

3.3.1 Separately Excited DC Motor

The external behavior of a separately excited motor is characterized by the equivalent circuit shown in Figure 3.2.

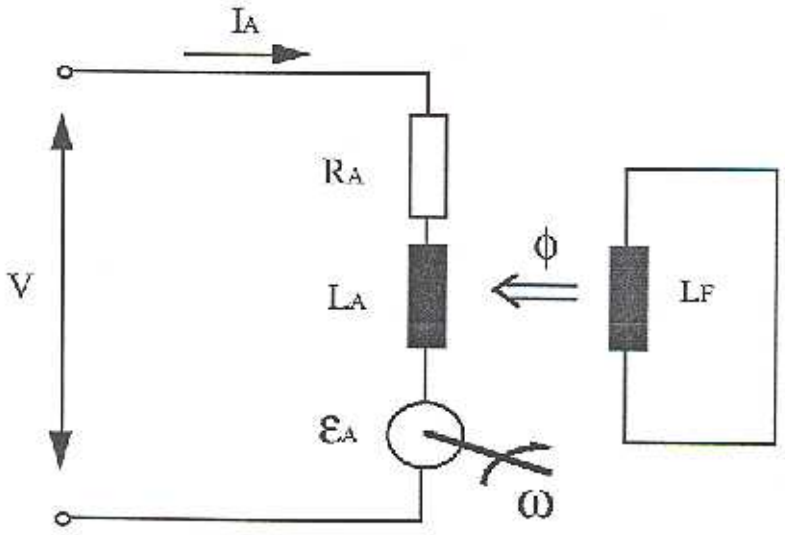

Figure 3.2 Separately excited motor equivalent circuit

The field source can be a permanent magnet or any other constant current source. A DC motor can be thought of as an ideal energy converter generating the *Electromotive force* (EMF), ε_A, in combination with parameters that represent its various imperfections. These parameters are, for the separately excited motor, the armature resistance, R_A, the inductance in the armature circuit, L_A, and the field inductance, L_F. The *EMF* induced in the armature windings is

$$\varepsilon_A = k \phi \omega \tag{3.3.1}$$

where k is the motor constant and ϕ is the magnetic flux.

If an energy source is connected to the motor terminal, a current I_A flows in the armature branch, and the electrical power generated is given by

$$P_{elec} = \varepsilon_A I_A = k \phi \omega I_A \tag{3.3.2}$$

Since the power is equal to the torque times speed, the electromagnetic or internal torque is given by

$$T = \frac{P_{elec}}{\omega} = k \phi I_A \tag{3.3.3}$$

The shaft torque is the difference between the ideal (electromagnetic) torque and the motor loss torque:

$$T_{shaft} = T - T_{loss} \tag{3.3.4}$$

As stated in the assumptions, the loss torque consists of a static friction and a dynamic friction component. The motor begins to start when it overcomes the static friction. At steady state, the terminal voltage of the motor is given by Kirchhoff's voltage law:

$$V_M = e_A + R_A I_A \tag{3.3.5}$$

The motor speed-torque characteristic is given by substituting equation (3.3.1) and equation (3.3.3) into equation (3.3.5). Rearranging to solve for the speed gives

$$\omega = \frac{V_M}{k\phi} - \frac{R_A T}{(k\phi)^2} \tag{3.3.6}$$

By coupling the motor to the PV array, the terminal voltage of the array is equal to the terminal voltage of the motor: $V_{PV} = V_M$ and the armature current is equal to the array current: $I_{PV} = I_A$. For each current-voltage pair of the array I-V curve the corresponding speed-torque (electomechanical torque) pair is obtained applying equations (3.3.3) and (3.3.6) simultaneously. The motor speed-torque characteristics at steady state are shown in Figure 3.3 for the mechanical plane (n, T) with $n = \omega/2\pi$ (n is in revolutions per minute, rpm). The n-T curves correspond to four different times of the day: a) 6am - Φ = 51 W/m^2, T_{amb} = 14.5°C; b) 8am - Φ = 319 W/m^2, T_{amb} = 13.9°C; c) 10am - Φ = 664 W/m^2, T_{amb} = 15°C, d) 12am - Φ = 963 W/m^2, T_{amb} = 16.7°C. The motor data are taken from reference [10] and are listed in Appendix C. For comparison, the figure also includes the motor n-T curve when it is supplied from a 130 V constant voltage source. The torque is a linear function of speed when the motor is supplied from a constant voltage source. The maximum torque, at constant irradiance, is obtained at starting conditions (n = 0) and it increases with increasing

irradiance. The no load speed (T = 0) is obtained for $I_A = 0$ and might be quite high even for low insolation levels.

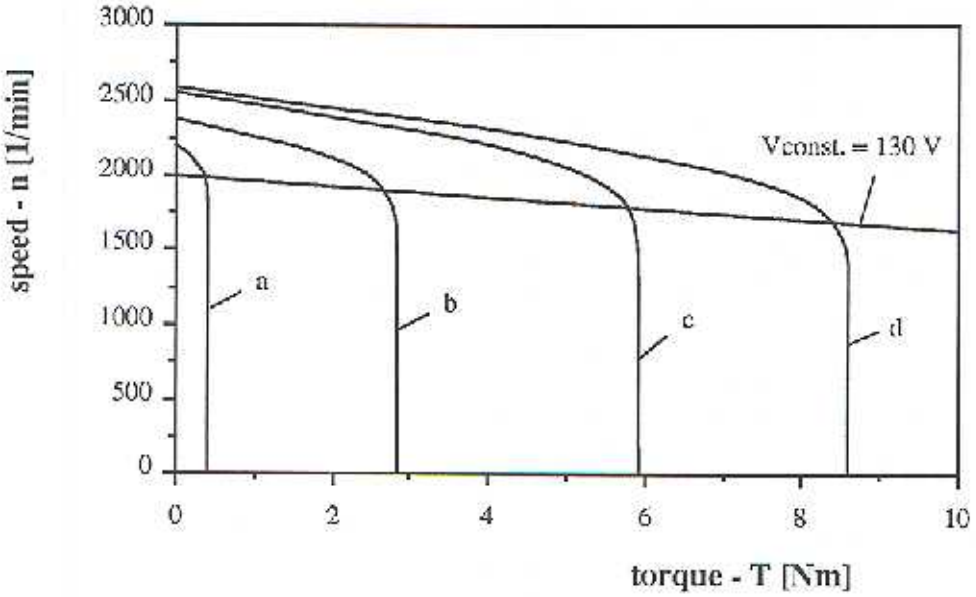

Figure 3.3 Separately excited motor speed-torque characteristics at different insolation levels. The n-T characteristics at a fixed voltage are also shown.

3.3.2 Series DC Motor

The equivalent circuit for a series motor is shown in Figure 3.4. The field windings are connected in series with the armature windings. Thus the terminal current is identical to the armature and field current:

$$I = I_A = I_F \tag{3.3.7}$$

and the internal resistance is the sum of the armature and field resistance:

$$R = R_A + R_F \tag{3.3.8}$$

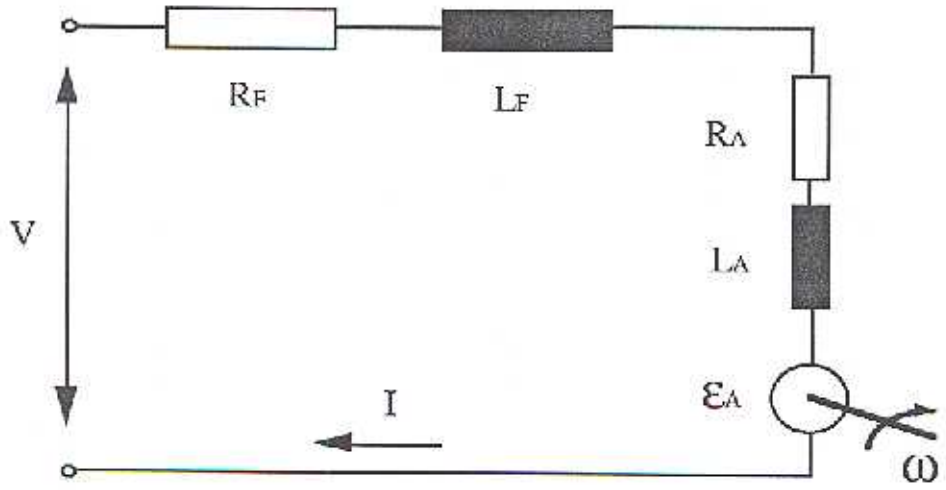

Figure 3.4 Series motor equivalent circuit

In contrast to the separately excited motor having a permanent magnet or a constant current field source, the magnetic flux of the series motor will vary with the terminal current. Magnetic flux and field current are related through a proportional factor, the constant k_F:

$$\phi = k_F I_F \tag{3.3.9}$$

Substituting this relation into equation (3.3.1) the *EMF* is expressed by

$$\varepsilon_A = k\, k_F\, I_F\, \omega = M_{AF}\, I\, \omega \qquad (3.3.10)$$

where the constants k and k_F are lumped together into the constant M_{AF}, called mutual inductance. Applying the same transformations to equation (3.3.3), the electromagnetic torque becomes

$$T = M_{AF}\, I^2 \qquad (3.3.11)$$

The terminal voltage is expressed similar to equation (3.3.5) by

$$V_M = \varepsilon_A + (R_A + R_F)\, I \qquad (3.3.12)$$

Finally the motor speed-torque characteristics may be found by substituting equations (3.3.10) and (3.3.11) in equation (3.3.12) and rearranging to solve for the speed:

$$\omega = \frac{V_M - R\sqrt{\frac{T}{M_{AF}}}}{\sqrt{T\, M_{AF}}} \qquad (3.3.13)$$

For a series motor directly coupled to a PV array, the speed-torque characteristics can be obtained in the same manner as described in section 3.3.1. For the same meteorological data as used for the separately excited motor (Figure 3.3), the n-T curves are shown in Figure 3.5. The n-T curve for the irradiance corresponding to 8am (a) is a straight line almost identical to the speed axis. The n-T curve for a 120V

constant voltage source is included for comparison which is in this case a parabolic function. The series motor has the same approximate nameplate rating as the separately excited motor. The actual data are listed in Appendix C.

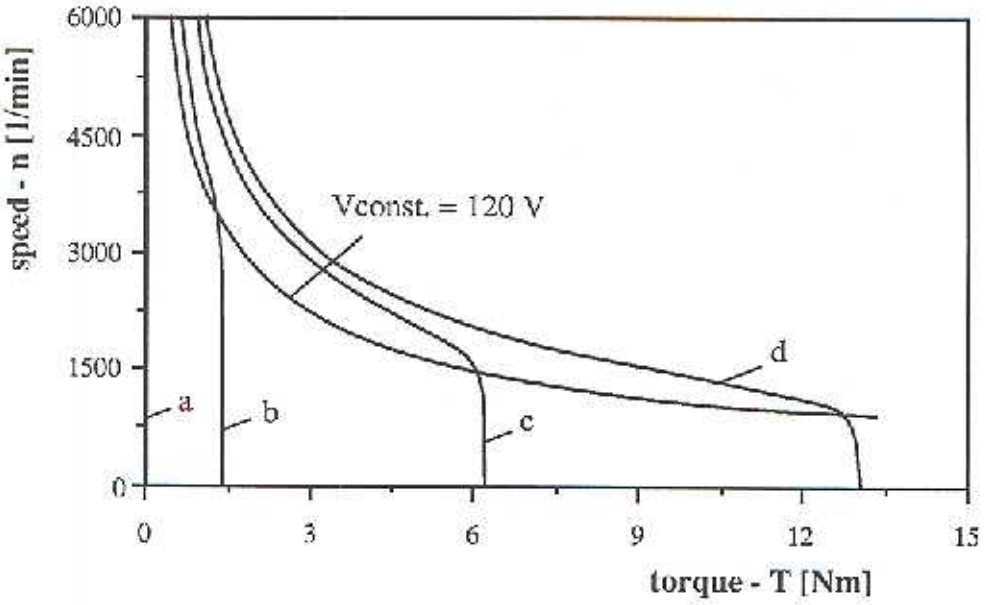

Figure 3.5 Series motor n-T characteristics at different insolation levels. The n-T curve at a fixed voltage is also shown.

Regarding the starting torque, the series motor behaves similar to the separately excited motor. At constant irradiance, the starting torque is at maximum torque and is increasing with increasing irradiance.

The speeds at no load, instead, are much higher than for the separately excited motor and may be higher than the maximum speed permitted. A series motor should never be operated without any load.

3.3.3 TRNSYS Component of the DC Motors

Both motors described above are integrated into the *TRNSYS* motor component. The information flow diagram for the component is shown in Figure 3.6.

The user can choose a motor by assigning a particular value to the parameter, TYPE, as explained above. I, V, Mode, n, and the shaft torque, T_{shaft}, serve as input. Either the current together with the speed or the voltage together with speed are significant inputs determined by the input, Mode. The torque and either voltage or current are computed respectively. As in the case of the resistance component, Mode has to be equal one for a direct coupled system, i.e. I and n are significant inputs, and Mode has to be zero for a system with battery storage, i.e. V and n are significant.

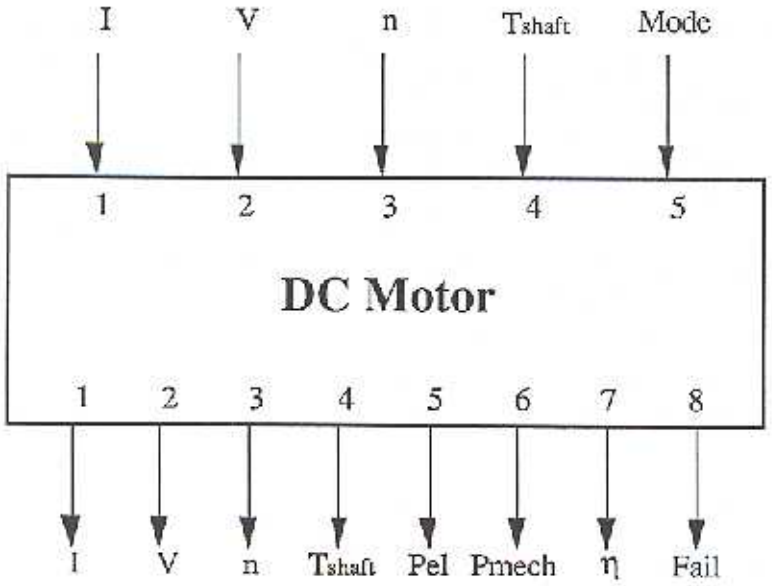

Figure 3.6 Information flow diagram of the DC motors component

The parameters of the component are:

1.) Type: if Type = 1 then the separately excited motor is used
if Type = 2 then the series motor is used

2.) N_{max} = maximum motor speed permitted [1/s]

3.) I_{rated} = rated current [amps]

4.) I_{max} = maximum current permitted [amps]

5.) k_F = motor constant for separately excited motor [Nm/amps]

or M_{AF} = mutual inductance for series motor [henry]

6.) C_{stat} = static friction [Nm]

7.) C_{visc} = viscous friction [Nm s]

8.) R_A = armature resistance [ohms]

9.) R_F = field resistance [ohms], just applicable for series motor

In Section 2.6, the iterative solution procedure of *TRNSYS* was explained and the convergence problem was discussed. A recyclic information flow between the PV array and any load is shown in Figure 2.9. In the case of motor loads, a recyclic information subloop is involved between the motor and the attached component (fan, pump, etc.). This means the operating point of the motor load has to be found by the *TRNSYS* iterative process. For instance, for a direct coupled system including a PV array, a motor and a fan, the motor component and the fan component are called sequentially until the speed and torque have converged for the current output from the PV array. This leads to a new voltage guess for the PV array and results in a different current that invokes again the motor subloop. This process is repeated until all inputs converge within a specified tolerance. The nature of the motor and load equations determine whether the method of successive substitution performed by *TRNSYS* will converge. For both motors, the fan and pump, convergence was not always obtained with the successive substitution method. Therefore, a convergence promoting algorithm was included in the motor component.

The first three iterations are performed using the regular *TRNSYS* method. Depending on the physical situation, the *secant* method or *bisection* method is used in the following iterations. Unless the particular situation occurs where the operating point in the mechanical plane is close to the boundaries, i.e. the torque axis, as shown in Figure 3.7, the convergence algorithm starts using the *secant* method converging on the torque output. The two most reasonable torque values from the previous iterations are used to find the new guess and the procedure is continued according to

$$x_{n+1} = x_n - \frac{g_n}{\frac{x_n - x_{n-1}}{g_n - g_{n-1}}} \qquad (3.3.14)$$

where x is equal to the torque and the objective function, g, is selected to be the difference between the recent and the previous torque. If either the residual, g increases or the new guess value is outside the limits which are set up at the first three iterations, it will be switched to the bisection method.

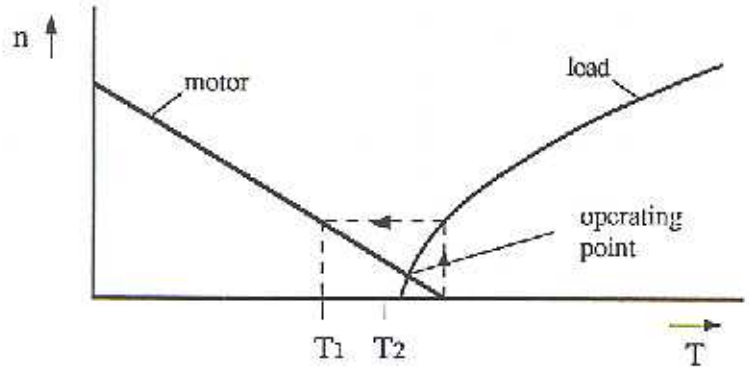

Figure 3.7 Illustration of the failure of the successive substitution method

For the situation illustrated in Figure 3.7, the bisection method is applied right away. This is a special situation where the successive substitution method would lead to an endless loop and the secant method might also fail. The separately excited motor equations, or more precisely the shaft torque-speed relation of the motor, is a straight line for a fixed current or fixed voltage. Depending on the slope of the motor line and the dimensions of the motor and the fan, especially the magnitude of the fan starting torque, the bisection method can yield two or more times a torque (indicated as T_1 and T_2 in Figure 3.7) that is less than the load starting torque. Thus the resulting load speed returned to the motor component is zero twice in sequence. Since the difference between the recent and the previous input is then zero, the convergence tolerance is satisfied and *TRNSYS* will stop calling the motor component and will hence generate an incorrect solution. To overcome this problem, the dummy input T_{shaft} is introduced.

TRNSYS will now converge on both variables, speed and torque.

Another problem is that the control function of the convergence promoting algorithm changes during a timestep. The motor relation changes quantitatively, i.e. the straight line is shifted, for each new current value received from the PV array. A similar problem arises in a system that contains a battery. If the battery has to be disconnected to protect it from undercharging, the significant inputs change from current to voltage. This will be explained in detail in Chapters four and five. This change requires that the limits for the convergence algorithm be reset to avoid an incorrect solution and the convergence algorithm will start over beginning with successive substitution every time the control function changes.

The outputs 5) and 6) are the electrical power input I times V, and the mechanical power output in watts corresponding to: $P = \omega T$. Output 7) is the motor efficiency. The last output contains following indication of failure:

Fail = 1: maximum permitted speed is exceeded

2: rated current is exceeded

3: maximum permitted current is exceeded

The maximum speed, the rated current and the maximum current are nameplate ratings and have to be provided as parameters. If the rated current is exceeded, the assumptions stated for the motor equations are not valid and the accuracy of the results will decrease. The program will not limit the values to the maximum permitted values if they are exceeded. This would be an interference in the iterative process of finding the operating point of the system and might lead to erroneous results.

3.3.4 Centrifugal Fan

The mechanical behavior of a ventilator can be expressed by the torque as a function of speed:

$$T = a + b\,\omega^c \tag{3.3.15}$$

where a is the static friction component and the remainder is a nonlinear function of speed. The actual data used in this study are taken from J.Appelbaum [10] and are listed in Appendix C. The parameters a, b, and c can either be obtained from manufacturers' data or from experimental data by performing a least square fit.

The motor-fan operation may be visualized in the mechanical n-T plane. Figure 3.8 shows the speed-torque characteristics for the separately excited motor connected to a fan.

The motor curves are drawn at the same conditions as presented in Figure 3.3. The load torque is the sum of the fan and the motor shaft loss torque and can be expressed by

$$T_{load} = T_{fan} + T_{loss} = a + C_{stat} + C_{visc}\,\omega + b\,\omega^c \tag{3.3.16}$$

The possible operating points of the motor-fan combination are located at the intersections of the motor and load lines. For the series motor-fan combination, the operation conditions are illustrated in Figure 3.9.

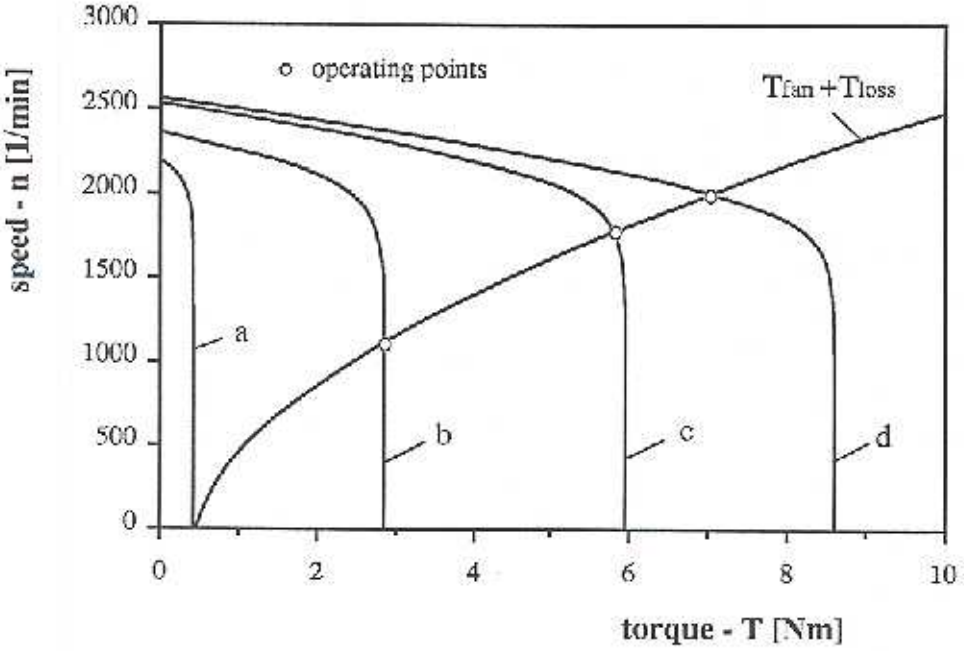

Figure 3.8 Separately excited motor and fan n-T characteristics

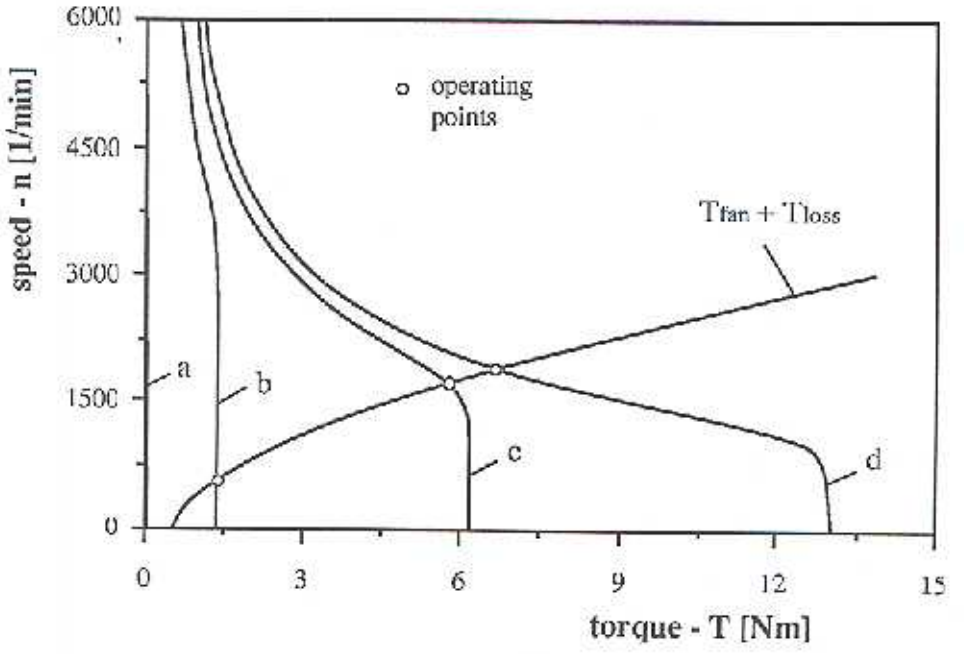

Figure 3.9 Series motor and fan n-T characteristics

From both Figures it can be observed that the fan starts only if a sufficient irradiance is available. The separately excited motor operates better at low insolation levels than the series motor.

The I-V characteristics are obtained by transforming all the possible operating points from the mechanical (n-T) plane into the electrical (I-V) plane using the motor equations presented in sections 3.3.1 and 3.3.2. Figure 3.10 shows the I-V curves for both the separately excited and the series motor. As already pointed out, both motors start when the radiation, i.e. the current and voltage, reaches a certain level. The starting points are indicated in the figure. Up to these points the motors act as ohmic resistances with straight lines in the I-V plane. Obviously, the series motor needs a significant higher starting current and higher voltage than the separately excited motor.

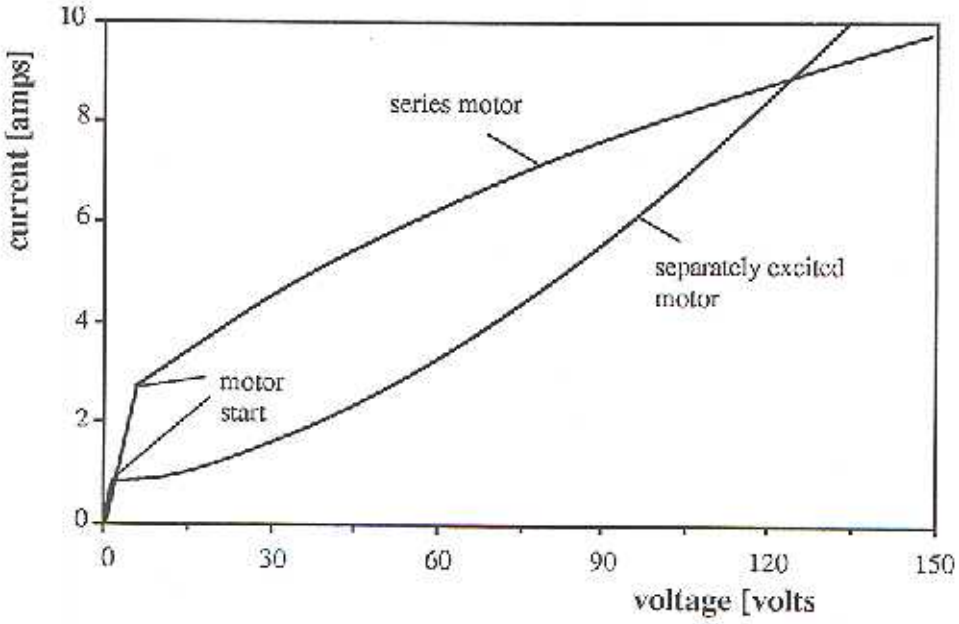

Figure 3.10 I-V characteristics of a separately excited and a series DC motor connected to a fan

3.3.5 TRNSYS Component of a Centrifugal Fan

As illustrated in Figure 3.11, the only input to the centrifugal fan component is the shaft torque provided from the motor. The speed, the shaft torque, the mechanical power and a failure message are outputs. The failure output is set equal to one when the fan speed exceeds the maximum permitted speed, otherwise it is zero.

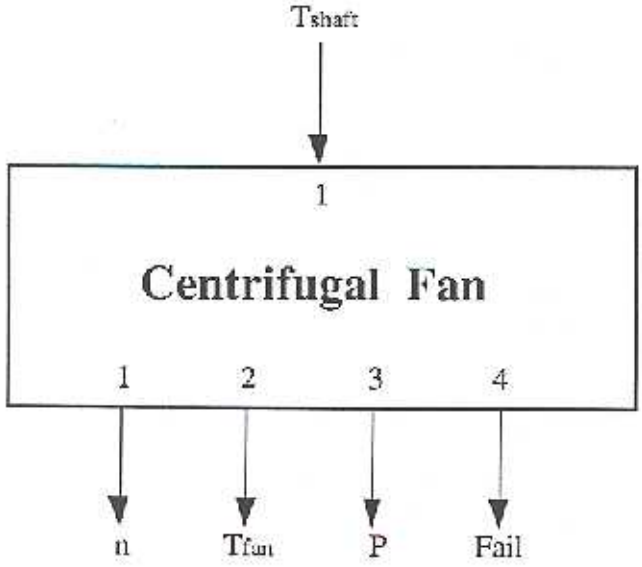

Figure 3.11 Information flow diagram of the fan component

The parameters of the component are:

1.) a

2.) b

3.) c

4.) N_{max} [1/s]

Parameters a,b and c are the constants of the torque speed relation (equation 3.3.15) where ω is substituted by n, and N_{max} is the maximum allowable fan speed.

3.3.6 Centrifugal Pump and Hydraulic System

The hydraulic part of a water pumping system consists of a pump and the piping system including valves fittings and so on. Typical PV water pumping applications are systems where water is pumped from open containments (sumps, wells, etc.) at low level to containments at high level, as shown in Figure 3.12. The model includes all the hydraulic components of such a system, including the pump.

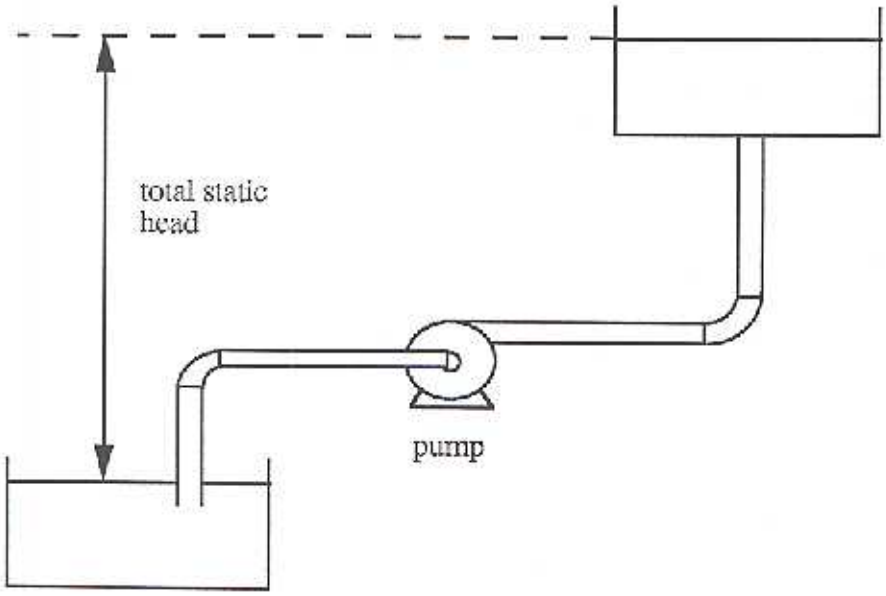

Figure 3.12 Water pumping system configuration

First the piping system is examined and a system head-capacity relation is derived. Then equations describing the centrifugal pump are developed using correlations from pump manufacturer data and fundamental pump relationships. The objective is to find the pump speed-torque relation, and in the same way it was attained for the ventilator, the pump I-V characteristics.

A typical head profile for a water pumping system is shown in Figure 3.13. The total static head is defined as the difference in height between the water supply surface and the water discharge level. The friction head is the required pressure difference expressed in meter liquid to overcome the friction caused in the piping system. The friction head is a function of flowrate.

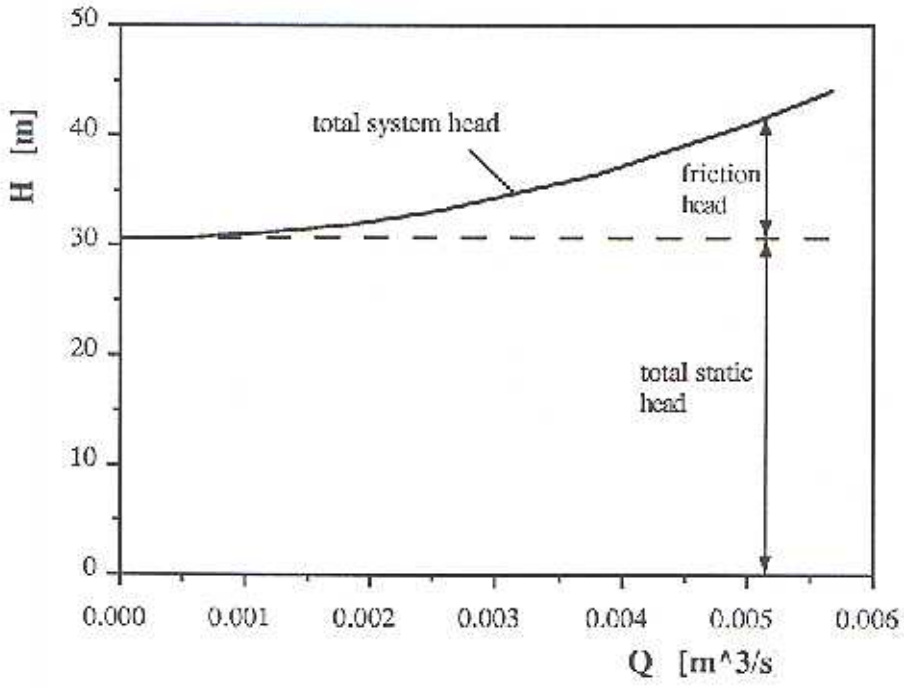

Figure 3.13 System head-capacity profile

The total system head is the sum of static and friction head and is expressed as

$$H_{syst} = k_1 + k_2 Q^2 \qquad (3.3.17)$$

where k_1 and k_2 are constants corresponding to the static and friction head, and Q is the system flowrate. The system head profile can either be obtained by measurements or

analytically by knowledge of the piping system components. The head loss for straight pipe is defined as

$$h_f = f \frac{L}{D} \frac{\overline{V}^2}{2\,g} \tag{3.3.18}$$

where

- f = friction factor
- L = length of the pipe [m]
- D = pipe diameter [m]
- $\overline{V}$ = average velocity [m/s]
- g = acceleration due to gravity [m/s^2]

The losses introduced by fittings, valves elbows, etc. are given by

$$h_f = K \frac{\overline{V}^2}{2\,g} \quad \text{with} \quad K = f \frac{L}{D} \tag{3.3.19}$$

K is the resistance coefficient and is available in related literature [16], [17], for a variety of piping components. The ratio L/D is the equivalent length in pipe diameters of straight pipe that will cause the same pressure drop as the valve or fitting under the same flow conditions and can be taken from tables and figures [16],[17]. The total head loss for the entire system is the sum of all head losses of the individual components.

Substituting the average velocity with the flowrate divided by the cross sectional area (A) this is

$$h_f = \sum_i \left(f \frac{L}{D} \frac{Q^2}{2 g A^2} \right)_i + \sum_j \left(K \frac{Q^2}{2 g A^2} \right)_j \qquad (3.3.20)$$

thus the coefficient k_2 in equation (3.3.17) may be obtained rearranging equation (3.3.20) and comparing the equation with the friction head in equation (3.3.17):

$$k_2 = \frac{1}{2 g} \left[\sum_i \left(f \frac{L}{D} \frac{1}{A^2} \right)_i + \sum_j \left(K \frac{1}{A^2} \right)_j \right] \qquad (3.3.21)$$

This method assumes an average friction factor.

The performance of a centrifugal pump is commonly visualized as head versus capacity characteristics. For a representative five horsepower pump, the performance curves are shown in Figure 3.14 as provided by a pump manufacturer. The performance curve combines the four variables: head, flowrate, speed and efficiency. Choosing any two variables fixes the remaining two variables. In the analysis and design of pumping systems, it is useful to superimpose the system characteristics on the pump characteristics as shown in Figure 3.15. The operating points are the intersections of the system curve and the pump curves. When a pump is started, first it operates along the head axis at zero flowrate until the system static head is reached. Then the flow starts and the actual operating point depends on the speed of the pump. For PV powered water pumping systems operation over the entire pump speed range is possible.

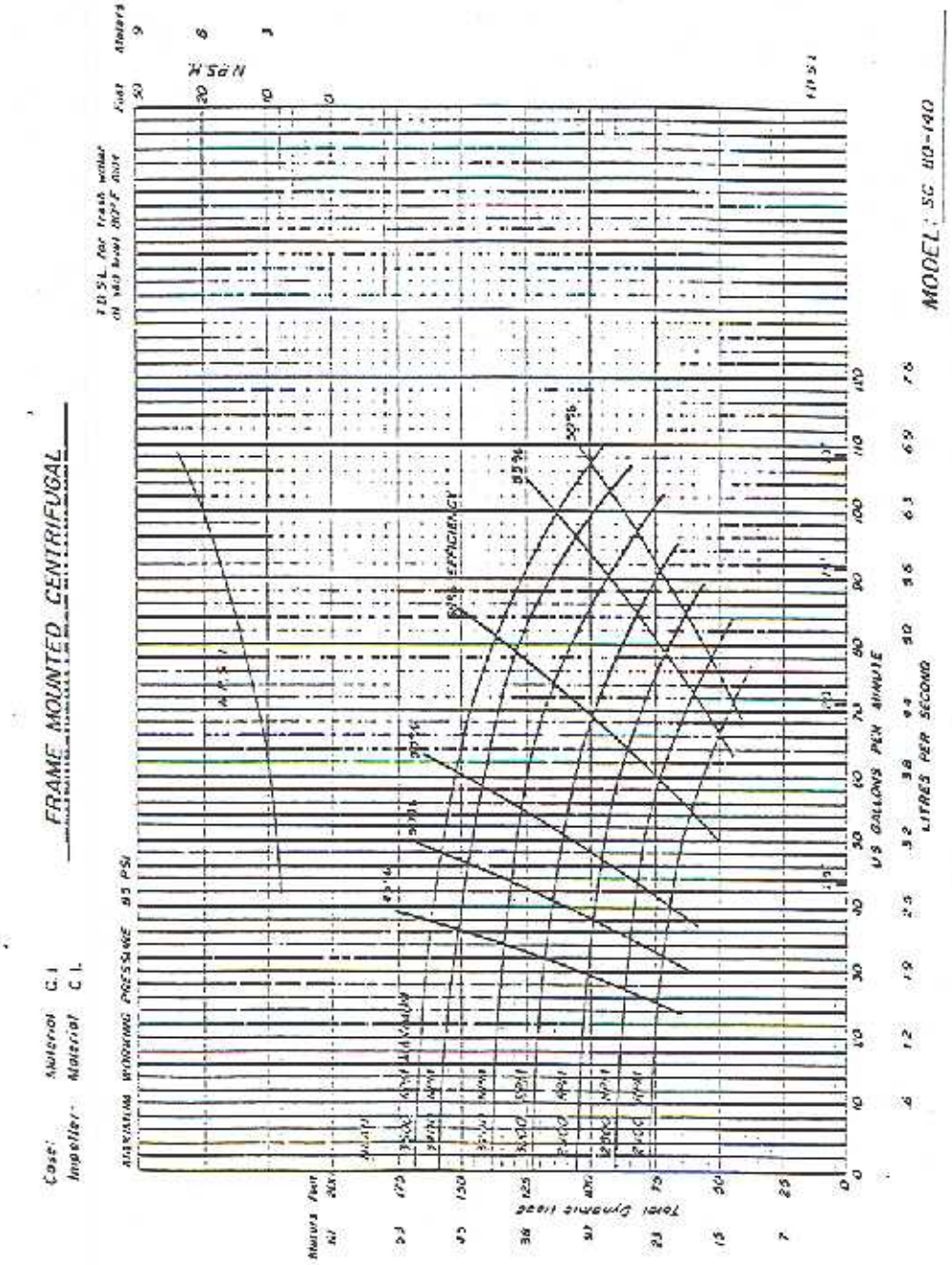

Figure 3.14 Centrifugal pump performance curve

To find the operating point of a pump, it is necessary to condense the pump performance data, provided by the manufacturer, into a useful equation. Fundamental pump laws supply the additional relationships required to obtain the pump speed-torque characteristics.

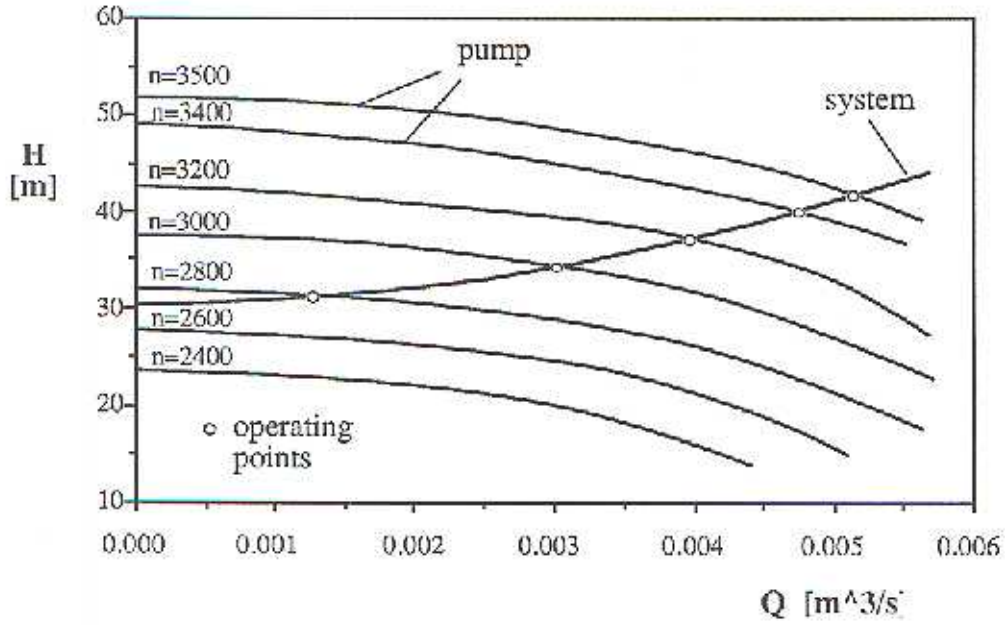

Figure 3.15 Pump performance curves (Model SC 80-140) and system head-capacity profile

From Figure 3.14 several pump features can be observed which are useful to find an appropriate relationship between head and capacity as a function of speed and efficiency. The head profiles are geometrically similar. This means that if the performance curve for one speed is known, it can be obtained for other speeds by moving the curve up or down [18]. The curves are theoretically moved along a parabola with the head axis as the main axis.

Further, the following *affinity laws* [19], which relate speed to flowrate, head and power, are applicable:

$$Q \sim n \quad \text{or} \quad Q = Q_1 \left(\frac{n}{n_1}\right) \tag{3.3.22}$$

$$H \sim n^2 \quad \text{or} \quad H = H_1 \left(\frac{n}{n_1}\right)^2 \tag{3.3.23}$$

$$P_{bh} \sim n^3 \quad \text{or} \quad P_{bh} = P_{bh1} \left(\frac{n}{n_1}\right)^3 \tag{3.3.24}$$

in which

n = speed [1/s]

n_1 = speed at which characteristics are known [1/s]

Q = flowrate [m^3/s]

Q_1 = flowrate at speed n_1 [m^3/s]

H = head [m]

H_1 = head at speed n_1 [m]

P_{bh} = brake horsepower [watts]

P_{bh1} = brake horsepower at speed n_1 [watts]

These equations imply that for a given set of speed, flowrate and brake horsepower, the corresponding values at a different speed can be determined for constant efficiency.

Forcing a curve through several values along the performance curve at a fixed constant speed, the pump head as a function of flowrate is well approximated by

$$H_1 = a_1 + b_1 Q_1^2 \tag{3.3.25}$$

To find the head-capacity relation at some other speed:

$$H = a + b\,Q^2 \tag{3.3.26}$$

the *affinity laws* can be used to substitute for H and Q and the following equation is obtained:

$$H_1 = a\left(\frac{n_1}{n}\right)^2 + b\,Q_1^2 \tag{3.3.27}$$

A comparison of the coefficients between equations (3.3.25) and (3.3.27) gives the coefficients at new speed:

$$a = a_1\left(\frac{n}{n_1}\right)^2 \qquad \text{and} \qquad b = b_1 \tag{3.3.28}$$

Given the head profile at a reference speed, it is now possible to attain the performance curve for any other speed. Since the affinity laws are valid for a moderate change in speed [19], an error will be introduced for large speed changes. However, even for large changes in speed, the error is acceptably low. Figure 3.16 shows the performance curves as supplied from manufacturer (Figure 3.14) and the curves generated with the method derived above. A second order least squares fit was performed through ten values from Figure 3.14 at a constant speed of 3000 rpm. As it can be seen, the approximation by equation (3.3.25) is quite good. For a speed of 3500 rpm, the modeled data and the manufacturer pump curve are compared. The maximum error is less than 2%.

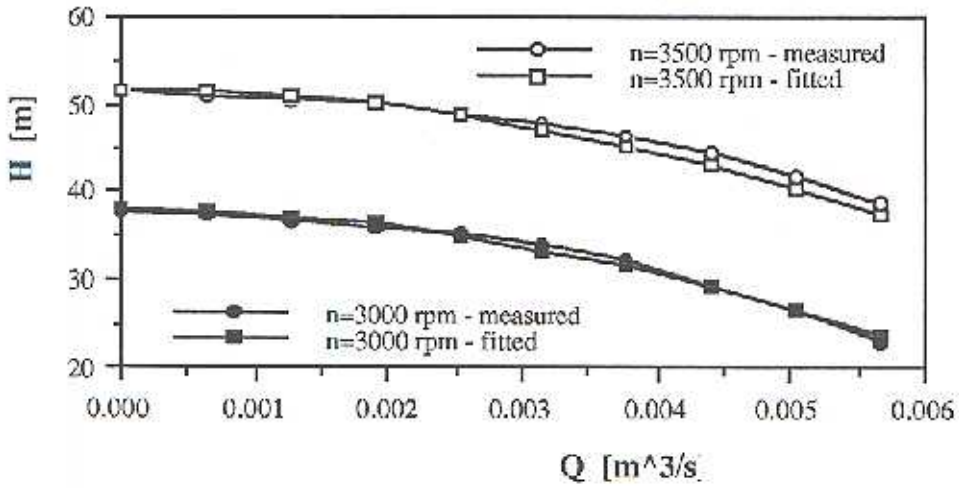

Figure 3.16 Comparison between measured and curve fitted head-capacity profile at two different speeds.

The pump operates at the point where the pump head is equal to the system head. Using equation (3.3.26) with the coefficients given by (3.3.28), the pump head curve is obtained; setting this equal to the system relation yields

$$H_{pump} = a_1 \left(\frac{n}{n_1}\right)^2 + b_1 Q^2 = k_1 + k_2 Q^2 = H_{system} \qquad (3.3.29)$$

This is one equation with two unknowns, n and Q. A second equation is given by the definition of the pump efficiency:

$$\eta = \frac{P_{hyd}}{P_{bh}} \qquad (3.3.30)$$

P_{hyd} is called the hydraulic power and is expressed as: $P_{hyd} = \rho\, g\, Q\, H$ and P_{bh} can be written as: $P_{bh} = 2\,\pi\, n\, T$. Substituting these expressions into equation (3.3.30), the efficiency is given as

$$\eta = \frac{\rho\, g\, Q\, H}{2\,\pi\, n\, T} \tag{3.3.31}$$

Two more unknown variables are introduced by this equation, the efficiency η and the torque T, therefore an additional relationship is necessary. Similar to the head profile, the efficiency profile at constant speed can be approximated by a polynomial. A good curve fit is attained by a cubic polynomial:

$$\eta = e_1 + f_1\, Q_1 + g_1\, Q_1^2 + h_1\, Q_1^3 \tag{3.3.32}$$

where e_1, f_1, g_1, h_1 are the coefficients at the given speed. The coefficients at other speed are determined applying the same procedure presented earlier and the efficiency relation can be rewritten as

$$\eta = e_1 + f_1\, n_1 \frac{Q}{n} + g_1\, n_1^2 \frac{Q^2}{n^2} + h_1\, n_1^3 \frac{Q^3}{n^3} \tag{3.3.33}$$

Substituting the head equation (3.3.26) for H in equation (3.3.31), equations (3.3.31) and (3.3.33) can be combined into a single equation. Together with equation (3.3.29) a system of two nonlinear equations is obtained:

$$a_1 \left(\frac{n}{n_1}\right)^2 + b_1\, Q^2 - k_1 - k_2\, Q^2 = 0 \tag{3.3.34}$$

$$e_1 + f_1\, n_1 \frac{Q}{n} + g_1\, n_1^2 \frac{Q^2}{n^2} + h_1\, n_1^3 \frac{Q^3}{n^3} - \frac{\rho\, g\, Q \left[a_1 \left(\frac{n}{n_1}\right)^2 + b_1\, Q^2\right]}{2\,\pi\, n\, T} = 0 \tag{3.3.35}$$

For a given torque, the system may be solved numerically using *Newton's method* [20]. Choosing the left hand side of equations (3.3.34-35) as the objective function $F(\vec{x})$, a *Taylor expansion* is performed, neglecting the higher order terms:

$$F(\vec{x} + \Delta\vec{x}) = F(\vec{x}) + J(\vec{x})\,\Delta\vec{x} \tag{3.3.36}$$

For the n-dimensional approach, a matrix is involved containing the derivatives of the objective function. The matrix is called the *Jacobian* matrix and is defined as

$$J(x) = \begin{bmatrix} \frac{\partial f_1(x)}{\partial x_1} & \frac{\partial f_1(x)}{\partial x_2} \\ \frac{\partial f_2(x)}{\partial x_1} & \frac{\partial f_2(x)}{\partial x_2} \end{bmatrix} \tag{3.3.37}$$

The objective is to minimize $F(\vec{x} + \Delta\vec{x})$, i.e. $F(\vec{x} + \Delta\vec{x}) = 0$. $\Delta\vec{x}$ is the difference between the new value and the value from the previous iteration. The new value is determined from equation (3.3.36) by:

$$\vec{x}_{n+1} = \vec{x}_n - J(\vec{x})^{-1}\,F(\vec{x}) \tag{3.3.38}$$

Newton's method requires the computation of the inverse of the *Jacobian* matrix. For the two-dimensional case, this can be done without solving a system of linear equations, using the following method [21]. If i is the ith row and k is the kth column the elements of the inverse *Jacobian* matrix are found by

$$[J]^{-1}_{ik} = \frac{P_{ik}}{|J|} \tag{3.3.39}$$

where P_{ik} is called the *cofactor* of the element $[J]_{ki}$, and $|J|$ is the determinant of J. P_{ik} is the determinant of the $(n - 1) \times (n - 1)$ submatrix of the $n \times n$ matrix J obtained by deleting the kth row and the ith column.

Newton's method converges quite fast (quadratic convergence), but it is very sensitive to the initial guesses. Initial guesses far from the solution may lead to erroneous solutions or the method may diverge. By using values from the previous timestep, the starting values are accurate enough.

Solving equations (3.3.34) and (3.3.35) for a given torque results in a flowrate and speed. The corresponding head is evaluated using equation (3.3.17) or (3.3.26) and the efficiency at the operating point may be computed applying (3.3.33). This technique is only valid for the operating range above the static head, i.e. beyond the point where flow begins. Below this point the affinity laws can be applied and the speed-torque characteristics are described by equation (3.3.24), substituting $2 \pi n T$ for P_{bh}:

$$T = T_1 \left(\frac{n}{n_1}\right)^3 \tag{3.3.40}$$

The torque-speed characteristics for the centrifugal pump for which the data are given in Figure 3.14 is shown in Figure 3.17. The flowrate versus torque is also shown. The static friction losses of the pump shaft are neglected. Up to the point where flow begins, the T-n curve is a parabola according equation (3.3.40). The I-V characteristics for the pump connected to either a separately excited or a series motor are shown in Figure 3.18. Point a) indicates the start of motor rotation, while b) indicates the beginning of flow.

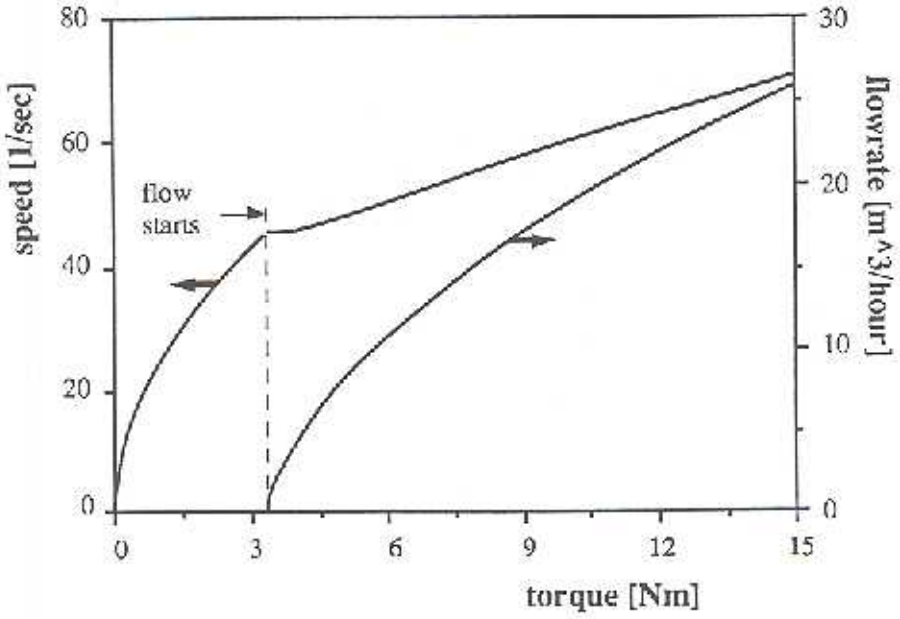

Figure 3.17 Pump n-T characteristics and flowrate versus torque curve

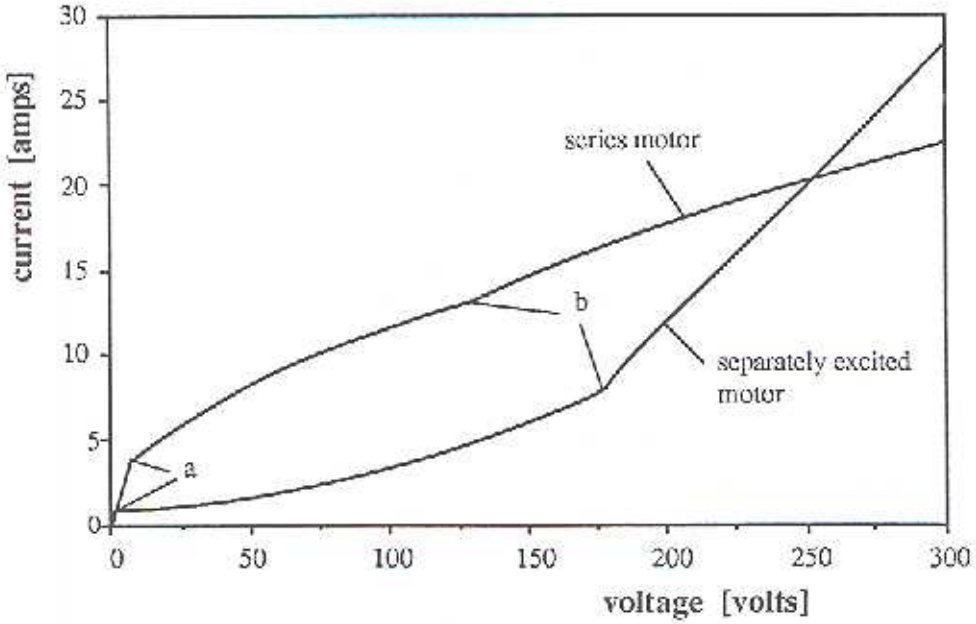

Figure 3.18 Motor-pump I-V characteristics. Point a indicates motor rotation start. Point b indicates begin of flow.

3.3.5 TRNSYS Component of a Hydraulic System

In addition to the single input, the shaft torque, and the parameters listed below, information about the pump performance at a given reference speed is also necessary to run the pump component. Two separate files must be provided by the user containing this information. The necessary data can be taken out of pump performance characteristics provided by manufacturer (e.g. Figure 3.14). One of the files must contain the head-capacity profile for a constant, i.e. reference speed. The user must supply several data pairs out of the head-capacity curve and to generate a file called "HEAD.DAT". The first row of this file must contain the number of data pairs. The following rows should contain the data pairs starting with the flowrate in cubicmeters per seconds followed by the head in meters. Flowrate and head must be separated by a space or comma. The second file, named "EFF.DAT", consists of the efficiency-capacity profile for a constant reference speed. Like the file "HEAD.DAT", the first row contains the number of data pairs and the following rows contain the data. The first column must be the flowrate followed by a space or comma and the efficiency. The program fits a curve through these data using the method of *Least Squares* [burden].

As shown in Figure 3.19, the outputs of the component are:

1.) n = speed [1/s]

2.) T_{shaft} = torque [Nm]

3.) Q = flowrate [m^3/s]

4.) H = head [m]

5.) η = efficiency

6.) P_{hyd} = water power [watts]

7.) P_{mech} = mechanical power [watts]

8.) Fail :1 = maximum pump speed is exceeded

:2 = newton method could not find reasonable solution

:3 = newton method did not converge within specified number of iterations

:4 = selected pump is to small to match system, i.e. speed required to provide flow is greater than the maximum permitted pump speed

If fail 3) occurs, the number of iterations needs to be increased in the component code. The pump speed will not be limited to the maximum speed when the pump speed exceeds the maximum pump speed, but the flowrate will be taken to be the flowrate at maximum speed permitted.

If no information about the power at shutoff condition is available, P_{off} has to be set equal to some negative number and it will be estimated. If it is available, it should be the power at the same reference speed which the files "HEAD.DAT" and "EFF.DAT" are based on. The constants k_1 and k_2 are the constants according to equation (3.3.17).

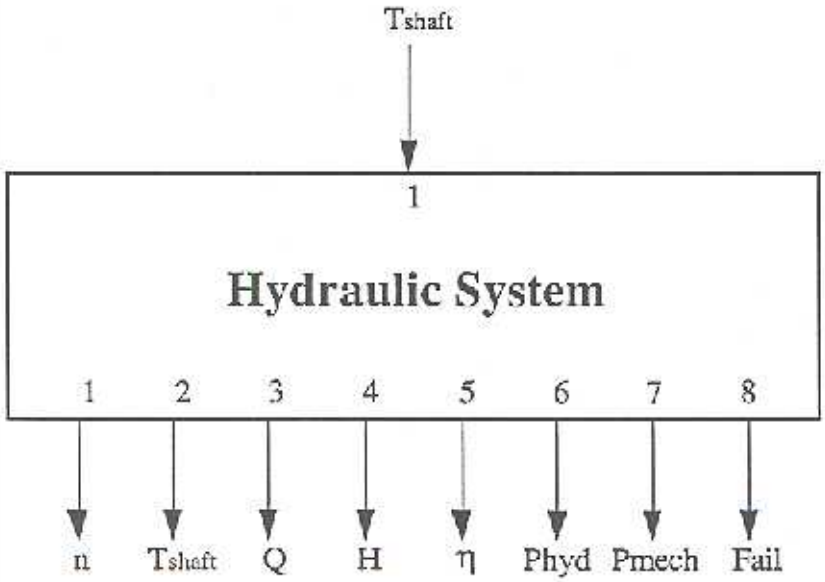

Figure 3.19 Information flow diagram of the hydraulic system component

The parameters of the component are:

1.) k1 = constant [m]

2.) k2 = constant [s^2/m^5]

3.) n_{ref} = reference speed [1/s]

4.) n_{max} = maximum pump speed permitted [1/s]

5.) P_{off} = shutoff power at reference speed [watts]

6.) Q_{nom} = nominal flowrate, the system is designed for [m^3/hour]

Chapter 4

BATTERY STORAGE AND MAXIMUM POWER TRACKING

Many operations require a continuous supply of energy and therefore the need of energy storage. A storage battery can be used for short term storage, that is for the use of energy during night time and time periods with low insolation. For energy transfer over long periods such as excess summertime solar energy to meet high wintertime energy demand, a battery is not an efficient tool. If a battery is selected to store photovoltaic energy, charge controllers are required to protect the battery from overcharge and excessive discharge.

Maximum power point tracking is used to maximize the power output of the PV array. This results in a reduction of expensive cell material and an increase in the economic value of the system.

This chapter includes a description of models of a battery, charge controllers, and a maximum power point tracker and a description of the *TRNSYS* components for these components.

4.1 BATTERY MODEL

The presented battery model is adopted from the already existing *TRNSYS* model [2] used by Evans et al. This model of a lead-acid storage battery was modified to operate with the components of a PV system presented in Chapter two and three. It provides a relationship between voltage, current and the *State of Charge* (SOC) of the battery. The model is a combination of the model developed by Shepherd [22] and that of Zimmerman and Peterson [23] as recommended by Hyman [24]. The equivalent circuit describing the isothermal DC battery cell behavior is shown in Figure 4.1.

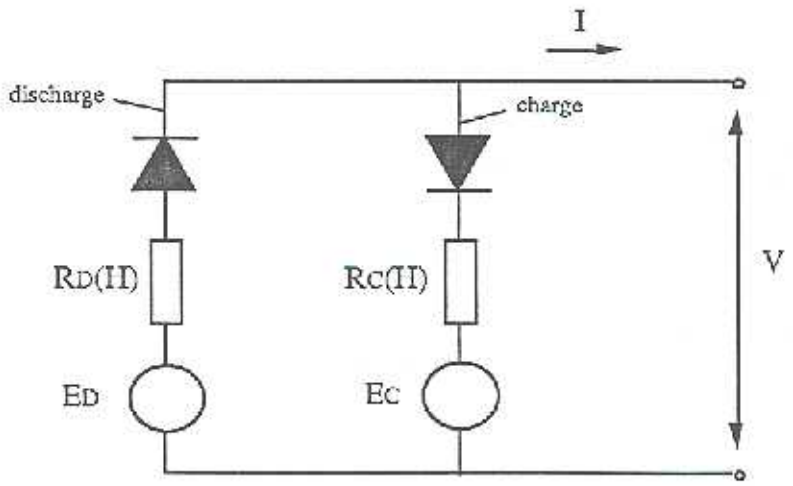

Figure 4.1 Equivalent circuit for a battery

The left leg is applicable on discharge and the right leg represents charge. The extrapolated open voltages, E_C on charge and E_D on discharge and the internal resistances, R_C and R_D, as functions of depth of discharge, H, were introduced by Shepherd. To take into account the behavior at very low current, Peterson and Zimmerman introduced the diodes. The formulas relating voltage, V, as a function of

current, I, and state of charge (or more precisely depth of discharge), are on discharge

$$V = V_{OC} - V_{DI} - G_D H + I R_{SD}\left(1 + \frac{m_D H}{\frac{Q_D}{Q_M} - H}\right) \tag{4.1.1}$$

and on charge

$$V = V_{OC} + V_{DI} - G_C H + I R_{SC}\left(1 + \frac{m_C H}{\frac{Q_C}{Q_M} - H}\right) \tag{4.1.2}$$

where

Q_M = rated capacity of cell

Q_C, Q_D = capacity parameters on charge, discharge

m_C, m_D = cell type parameters which determine the shape of the I-V-capacity characteristics

R_{SC}, R_{SD} = internal resistances at full charge when charging, discharging

H = fractional depth of discharge

G_C, G_D = small-valued coefficients of H

The fractional state of charge of a battery can be expressed as the ratio of actual capacity (Q = SOC) and rated capacity.

$$F = \frac{Q}{Q_M} \tag{4.1.3}$$

The fractional depth of discharge is then: H = 1 - F.

The open circuit voltage may be expressed as

$$V_{OC} = \frac{E_{SC} + E_{SD}}{2} \tag{4.1.4}$$

where E_{SC} and E_{SD} are the constant open circuit voltages, extrapolated from V versus I curves on charge and discharge at fully charged battery. The voltage drop at the diodes is characterized by

$$V_{DI} = \frac{1}{K_{DI}} \ln\left(\frac{|I|}{I_{DI}} + 1\right) \tag{4.1.5}$$

where K_{DI} and I_{DI} are curve fitting parameters.

The internal resistances in equations (4.1.1) and (4.1.2) are expressed by R_{SC} and R_{SD} times the following term in brackets

$$R(H) = R_{S(C,D)}\left(1 + \frac{m_{C,D}\, H}{\frac{Q_{C,D}}{Q_M} - H}\right) \tag{4.1.6}$$

When the cell is fully charged (H = 0), the internal resistance of the cell is equal to R_{SC} or R_{SD}. As discharge proceeds the internal resistance increases and thus the voltage drop increases.

The I-V characteristics described by equations (4.1.1) and (4.1.2) for four different state of charge levels are shown in Figure 4.2. The voltage scale is expanded for better resolution.

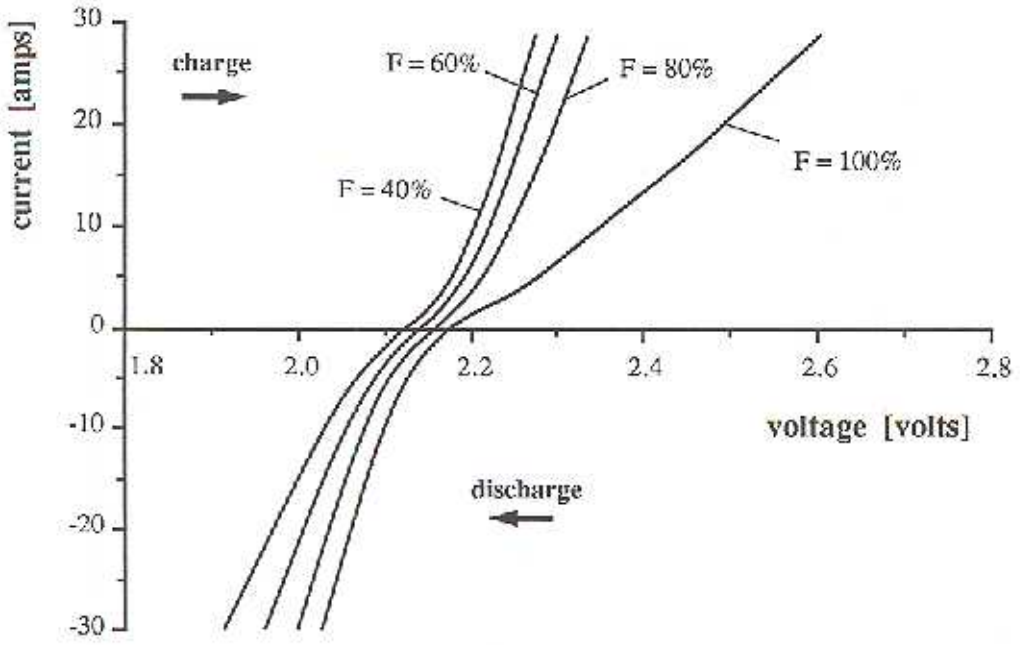

Figure 4.2 Lead acid battery I-V characteristics for a 250 ampere hour rated capacity, single cell at different levels of state of charge (F in %)

At fixed H, the voltage increases almost linearly with the charge current and decreases almost linearly with the discharge current. The effect of the diode is only significant at low currents where the curves have an exponential behavior. The battery terminal voltages on charge is higher than on discharge. The voltage decreases with decreasing SOC.

The variation of SOC with respect of time may be determined on discharge:

$$\frac{dQ}{dt} = I \qquad \text{with } I \le 0 \qquad (4.1.7)$$

and on charge

$$\frac{dQ}{dt} = I\,\eta \qquad \text{with } I > 0 \qquad (4.1.8)$$

where Q is the state of charge in ampere-hours and η is the charging efficiency. The charging efficiency takes into account that some of the charging current is wasted in producing gas and various other losses. The efficiency is assumed to be constant.

The presented model does not include the effects of temperature, battery self discharge and battery aging. Battery aging refers to the number of charge-discharge cycles the battery has undergone. Self discharge can be neglected in PV applications where the battery is continuously operated. The capacity loss due to self discharge is equalized frequently by charging the battery with excess PV energy.

4.2 TRNSYS COMPONENT OF A BATTERY

The information flow diagram of the battery component is shown in Figure 4.3. The only input of the component is the current. The equations presented in section 4.1 are valid for a single battery cell. The battery may consist of several cells connected in series and parallel to satisfy the voltage and current requirements of the load. The relations between the current and voltage for a single cell and the entire battery are as follows:

$$I_{B,tot} = CP\ I_{B,cell} \tag{4.2.1}$$

$$V_{B,tot} = CS\ V_{B,cell} \tag{4.2.2}$$

where CP is the number of cells wired in parallel and CS is the number of cells wired in series. CP and CS can be specified as parameters by the user. These relations are used for all currents and voltages serving as input and outputs.

The output voltages V_D and V_C are the voltage limits on discharge and charge for possible use in the charge controllers. The battery component does not limit any operating condition. All the restrictions concerning the battery protection must be done in the charge controllers. To avoid battery damage, the battery must be protected from overcharge and deep discharge. Charging the battery to too high a voltage causes gassing which reduces the charging efficiency and there is a danger of explosion from the generated hydrogen and oxygen gases. In practice, one does not discharge a battery below a certain voltage. Cell voltage decreases almost linearly with depth of discharge until a point is reached where the voltage drops more rapidly and exhaustion of the cells is reached. Further discharge is not economical and may result in permanent damage. V_C, and V_D, have to be provided by the user for a single cell. Data are available in battery handbooks or can be obtained from manufacturer. While V_C is assumed to be constant, a relation determining V_D as a function of the discharge rate, as provided by Hyman [24] can be used:

$$V_D = E_D - |I| R_D \tag{4.2.3}$$

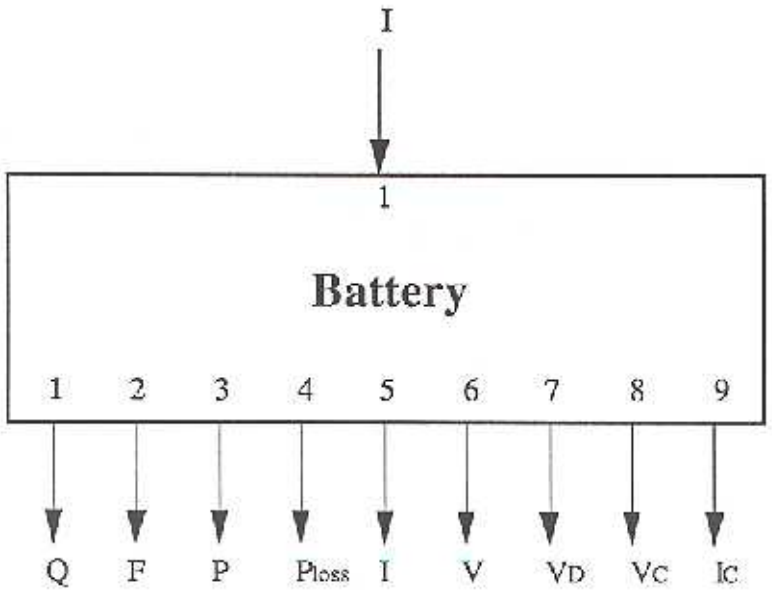

Figure 4.3 Information flow diagram of the battery component

The parameters of the components are

1.) Q_M [Ah]
2.) CP
3.) CS
4.) η
5.) V_C [V]
6.) V_D [V]
7.) $I_{C,TOL}$
8.) E_{SC} [V]
9.) E_{SD} [V]
10.) G_C
11.) G_D
12.) M_C
13.) M_D
14.) E_D [V]
15.) R_D [ohms]
16.) I_{DI} [amps]
17.) K_{DI}
18.) Q_C [Ah]
19.) Q_D [Ah]
20.) R_{SC} [ohms]
21.) R_{SD} [ohms]

This relation is used if parameter 6) is set equal to a negative value. If a constant value for V_D is desired, parameter 6) has to be set equal to this constant value. The current I_C corresponding to V_C is an output and can be used by the charge controllers. The output P_{loss} is the wasted energy during charge and is evaluated as

$$P_{loss} = (1 - \eta) P \tag{4.2.4}$$

where P is the input power to the battery.

Parameters 1 to 3 determine the size of the battery. The current I_C has to be evaluated numerically, since equation (4.1.2) is an implicit relation for the current. Parameter 7 is an absolute tolerance which determines the accuracy of the evaluation of I_C. The remaining parameters are battery dependent. A set of parameters for a lead acid battery is provided in Appendix C. The parameters are taken from the TRNSYS component code [2] and are originally from Hyman which he derived from data of Vinal [25].

4.3 CHARGE CONTROLLERS

Charge control is inevitable when using battery for energy storage in PV systems. The battery must be protected from overcharge and deep discharge or damage of the battery may result. Two standard types of charge controllers have been modeled and will be presented in the following sections: A simple voltage and SOC limiter for array and

load shedding which is a series type charge controller. Secondly a more sophisticated shunt type controller which has a multiple step control scheme.

SOC depends on many factors and is difficult to measure. Estimation of the state of charge of a battery is usually done by sensing the battery terminal voltage. More sophisticated controllers also have ampere-hour accumulators which provide a more accurate picture of the state of charge of the battery [26],[6],[27]. Both controllers presented in this thesis incorporate voltage sensing and ampere-hour accumulation. The state of charge of the battery is actually evaluated in the battery component using equations (4.1.6) and (4.1.7).

4.3.1 Series Type Charge Controller

The system configuration of a PV system with battery storage and a series type charge controller is shown in Figure 4.4.

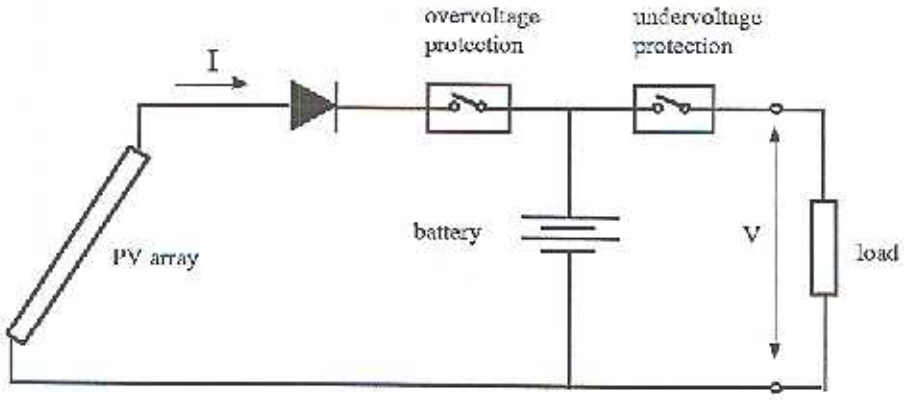

Figure 4.4 PV system with battery storage and a series type charge controller

The controller consists of two main devices: the overvoltage protection and the undervoltage protection. In the simplest version of this type of charge controller, as it is implemented in the TRNSYS component, relays turn off the current to or from the battery when it is necessary. When either the state of charge of the battery or the voltage exceeds the charge limits specified by the user, the array will be disconnected from the battery and the load. The upper limit for the voltage is the voltage at which severe gassing occurs. The battery is then discharged through the load. On discharge, the controller will disconnect the load from the battery when either the battery voltage drops below the cutoff voltage or the state of charge is less then the allowed final state of charge. The battery will then be recharged from the array. This strategy attempts to keep the battery at the appropriate charge level rather than satisfying the load.

The diode between the array and the battery prevents the battery from being discharged through the array during the night.

4.3.2 TRNSYS Component of a Series Type Charge Controller

Besides the terminal battery voltage, V_B, and the terminal battery current, I_B, the controller takes the fractional state of charge, F, the gassing voltage, V_C, and the cutoff voltage on discharge, V_D, from the battery component. The information flow diagram is shown in Figure 4.5

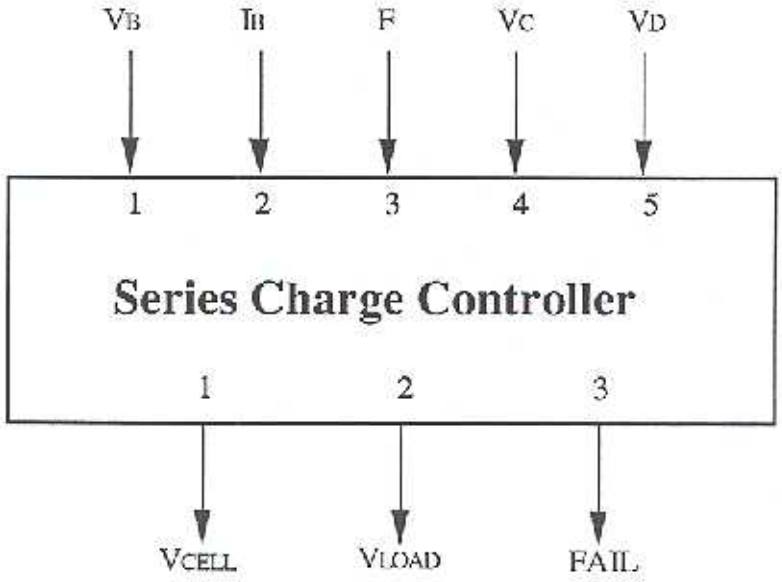

Figure 4.5 Information flow diagram of the series type charge controller

The parameters of the component are:

1.) F_D = discharge limit on state of charge

2.) F_C = charge limit on state of charge

3.) F_{DA} = state of charge above battery can be discharged again after being charged

4.) F_{CA} = state of charge below battery can be charged again after being discharged

5.) V_{DA} = voltage above battery can be discharged again after being charged [V]

6.) V_{CA} = voltage below battery can be charged again after being discharged [V]

7.) $I_{B,MAX}$ = maximum battery current permitted [amps]

8.) $I_{B,MIN}$ = minimum battery current permitted [amps]

9.) V_{DIODE} = voltage drop at the diode [V]

F_D and F_C are the state of charge limits on charge and discharge. F_{DA}, F_{CA}, V_{DA}, V_{CA} are constraints describing a dead band which prevents the controller from oscillating between the operating states. When the battery voltage reaches the gassing voltage or the upper limit of SOC, the battery will be discharged at least to the limits F_{CA} and V_{CA} before it can be charged again.. The same is valid for the limits on discharge. These limits have to be determined very carefully. The performance of the entire PV system might suffer if the dead band is chosen to large, because the load might be disconnected from the battery and the array longer than required. Setting the limits requires some knowledge about the behavior of the entire system. The voltage limits V_{CA} and V_{DA} must be specified for the entire battery and not just for one cell as it is the case for the battery parameters V_C and V_D. The operating range of the battery and the dead bands after charge and discharge are illustrated in Figure 4.6. The I-V curves for six different SOC levels are shown. All the limits are chosen arbitrarily.

The outputs of the controller are the voltage to the PV array, V_{CELL} and the voltage to the load, V_{LOAD}, and a message, FAIL, announcing possible failure operation conditions. V_{CELL} differs from V_{LOAD} which is equal to the battery terminal voltage to the voltage drop across the diode. The diode voltage drop is assumed to be constant which is adequate for currents greater then milliamperes. For a silicon diode the voltage drop is approximately 0.7 volts.

Fail equal to one means that the discharge current is greater than maximum current permitted. Fail equal to two means that the maximum charge current of the battery is exceeded. The controller does not constrain the current. The failure message is the only precaution performed to inform the user that the battery or other system components have been designed incorrectly.

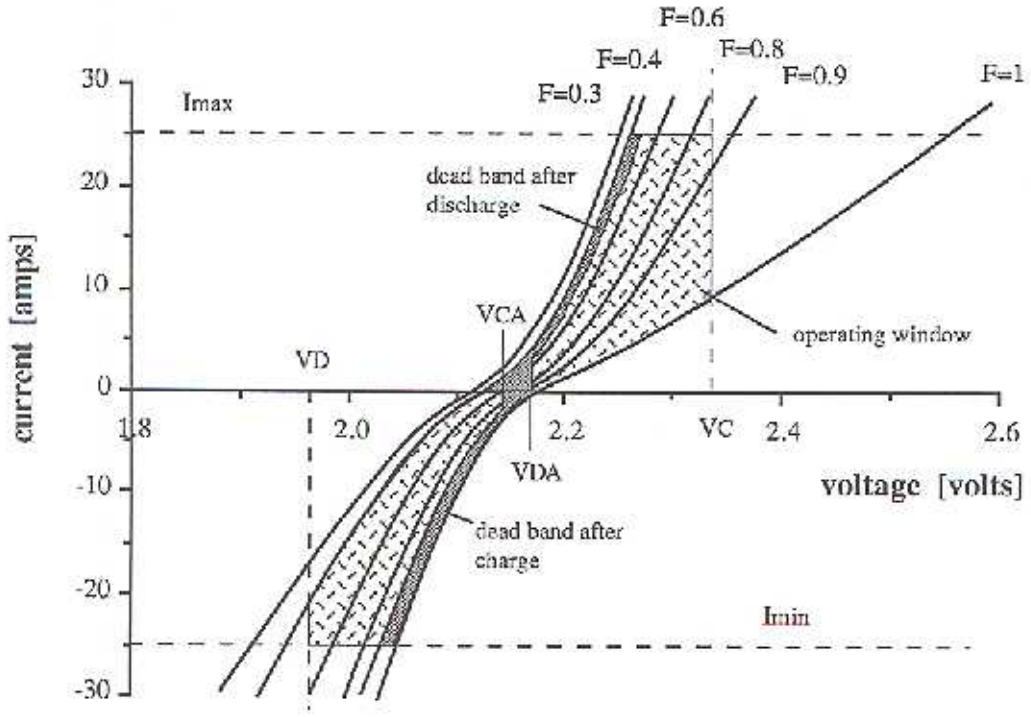

Figure 4.6 Illustration of the battery operation limits

To illustrate how a PV system, as shown in Figure 4.4, can be simulated using *TRNSYS*, an information flow diagram can be drawn as shown in Figure 4.7. All the important individual components and their interconnection are shown. The direction of the information flow is indicated through arrows. The load could be any kind of electrical load.

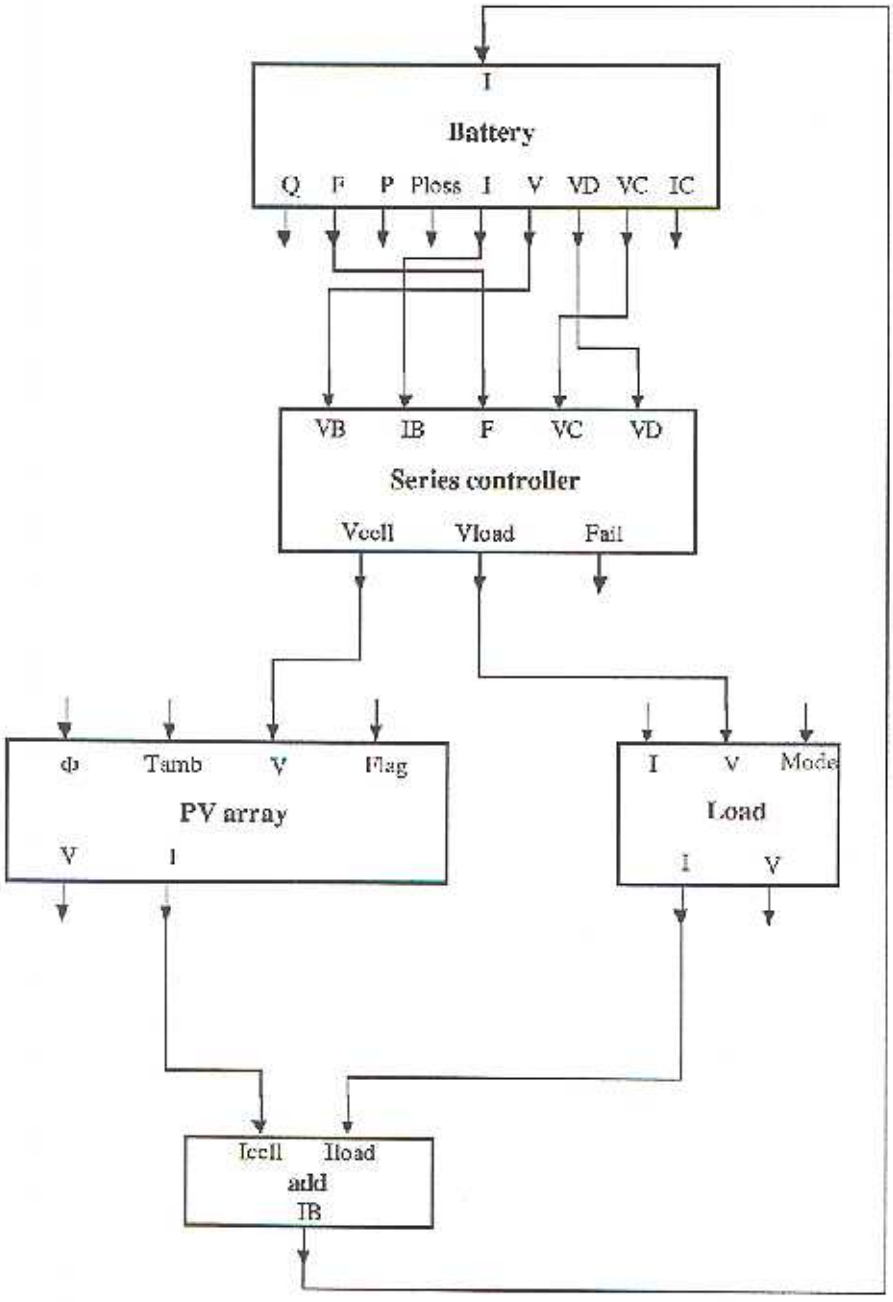

Figure 4.7 TRNSYS system configuration of a PV system including battery storage and a series type charge controller

In such a system,the operating voltage range is determined from the battery voltage. Although the battery terminal voltage varies, as discussed earlier in this chapter, the variation is relatively small. The battery acts almost like a voltage regulator. Therefore the battery should be the first component of the PV system called from *TRNSYS*. The charge controller receives the battery voltage and does the F and V checks as already explained. In the normal operating mode, where the battery voltage and SOC are within the limits, the controller does not interfere. The cell voltage differs from the battery voltage by the magnitude of the voltage drop of the diode:

$$V_{CELL} = V_{DIODE} + V_B \tag{4.3.1}$$

The voltages shifted to the PV array and the load generate currents which are transferred to a hypothetical device called add. This device determines the battery current according to Kirchhoff's current law:

$$I_B = I_{CELL} - I_{LOAD} \tag{4.3.2}$$

Add can be realized in *TRNSYS* using the Equation card [2]. The current I_B is then returned to the battery and the process is continued until the convergence tolerance is satisfied, and the operating point is found. When the battery reaches a charge level which requires the disconnection of the load from the battery, the controller sets the output V_{load} equal to zero. That results in a battery current equal to the PV array current indicating that the battery is now being charged from the array.

On the other hand, if the battery is fully charged and the array needs to be disconnected, the controller sets the output V_{cell} to some negative value. The resulting battery current is now equal to the negative load current, and the battery is being discharged from the load.

4.3.3 Shunt Type Charge Controller

The shunt type charge controller discussed in this section differs fundamentally from the series type controller presented above. The shunt type controller is a voltage regulator rather than a voltage limiter as the series type controller is. Furthermore the shunt type controller has its priority on satisfying the load rather than keeping the battery on a high level of SOC. The system configuration including a PV array, a battery, a shunt type controller, and a load is shown in Figure 4.8.

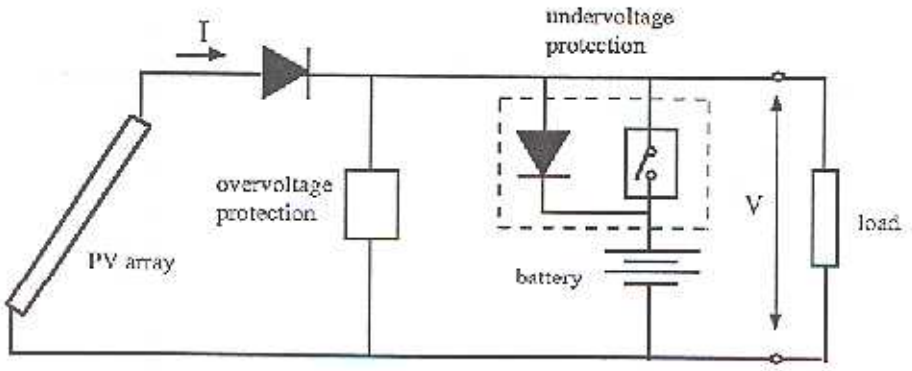

Figure 4.8 PV system with battery storage and shunt type charge controller

The overvoltage protection consists basically of a dissipative device. When the battery is fully charged or when the battery voltage would exceed the gassing voltage, the current into the battery is reduced by shunting current through the overvoltage protection branch. The power involved with this current is dissipated which is technically realized using Zehner diodes, transistors, or a bank of resistances [26]. A disadvantage is the generated heat in these power dissipation devices.

Deep discharge is prevented by disconnecting the battery from the load. When the battery SOC or the cutoff voltage on discharge would be exceeded the current flow out of the battery is turned off (see undervoltage protection in Figure 4.8). This is equivalent to the operation of a direct coupled system, such as a system without battery storage. The diode in the undervoltage protection device, acts as a valve and allows the battery to be charged from the array when the array produces more energy than the load requires, while the switch is turned off. This control scheme prefers satisfying the load rather than recharging the battery.

4.3.4 TRNSYS Components of a Shunt Type Charge Controller

The task of modeling the shunt type controller is realized in two different TRNSYS components: part A and part B. At first the similarities of both components will be described. In order to understand the selected inputs and outputs of these components it is necessary to look at the configuration and the information flow of an entire PV system as it is would be implemented in TRNSYS.

Shunt Type Charge controller: Part A

The information flow diagram of the component is shown in Figure 4.9. The inputs are the same as for the series type controller except for the two additional inputs V_{load} and Guard. V_{load} is the voltage taken from the load component, and Guard is a signal received from the shunt controller part B.

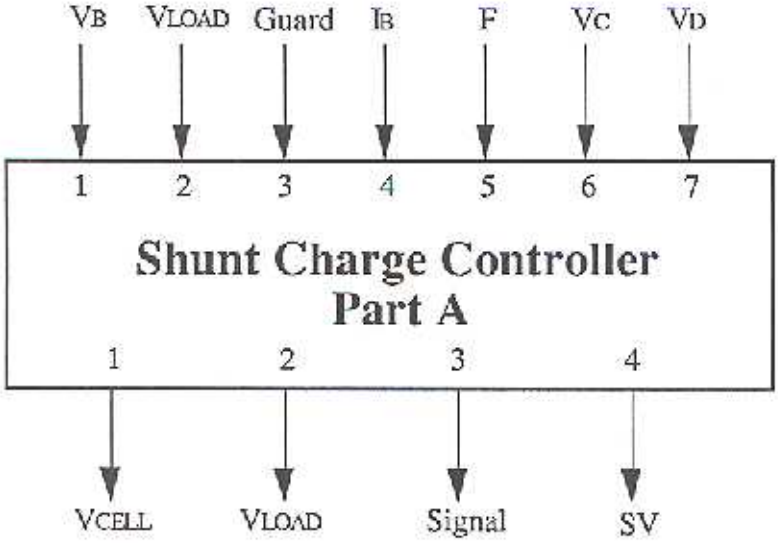

Figure 4.9 Information flow diagram of the shunt type charge controller part A

The parameters of the component are:

1.) V_{DA} [V]

2.) F_D

3.) F_C

4.) F_{DA}

5.) F_{CA}

6.) V_{DIODE} [V]

These parameters have already been explained for use in the series controller. V_{DIODE} stands for the voltage drop of both diodes incorporated in the controller.

The outputs are the voltage to the PV array, V_{cell} and the voltage to the load, V_{load}. The remaining inputs are control signals: Signal is for possible use in the PV array and the load, and SV is for the use in the shunt controller part B.

Shunt Type Charge controller: Part B

The inputs for this component are the battery current and voltage, I_B and V_B, the upper limit on voltage and the corresponding current, V_C and I_C, and a control signal, SV, as shown in Figure 4.10.

As outputs, the battery current, I_B, a signal, Guard, the dissipated power, Pdiss, and a failure message, Fail, have been selected. Fail reports if the battery current limits are exceeded: Fail = 1 means that the maximum discharge current is exceeded and Fail = 2 means the the maximum charge current is exceeded. As with the series controller, the current will not be restricted to its limits. The failure message is the only precaution taken to show the user that the battery or other system components have not been properly designed.

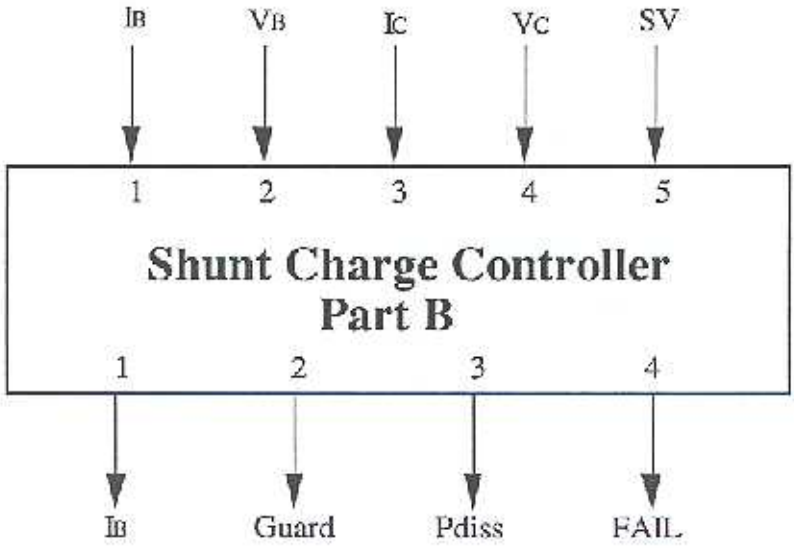

Figure 4.10 Information flow diagram of the shunt type controller part B

The parameters of the components are:

1.) $I_{B,MAX}$ = maximum battery charge current permitted [amps]

2.) $I_{B,MIN}$ = minimum battery discharge current permitted [amps]

The information flow diagram of a PV system using the shunt controller is more complex than that for the system using the series type controller. All the important individual components and their interconnections are shown in Figure 4.11.

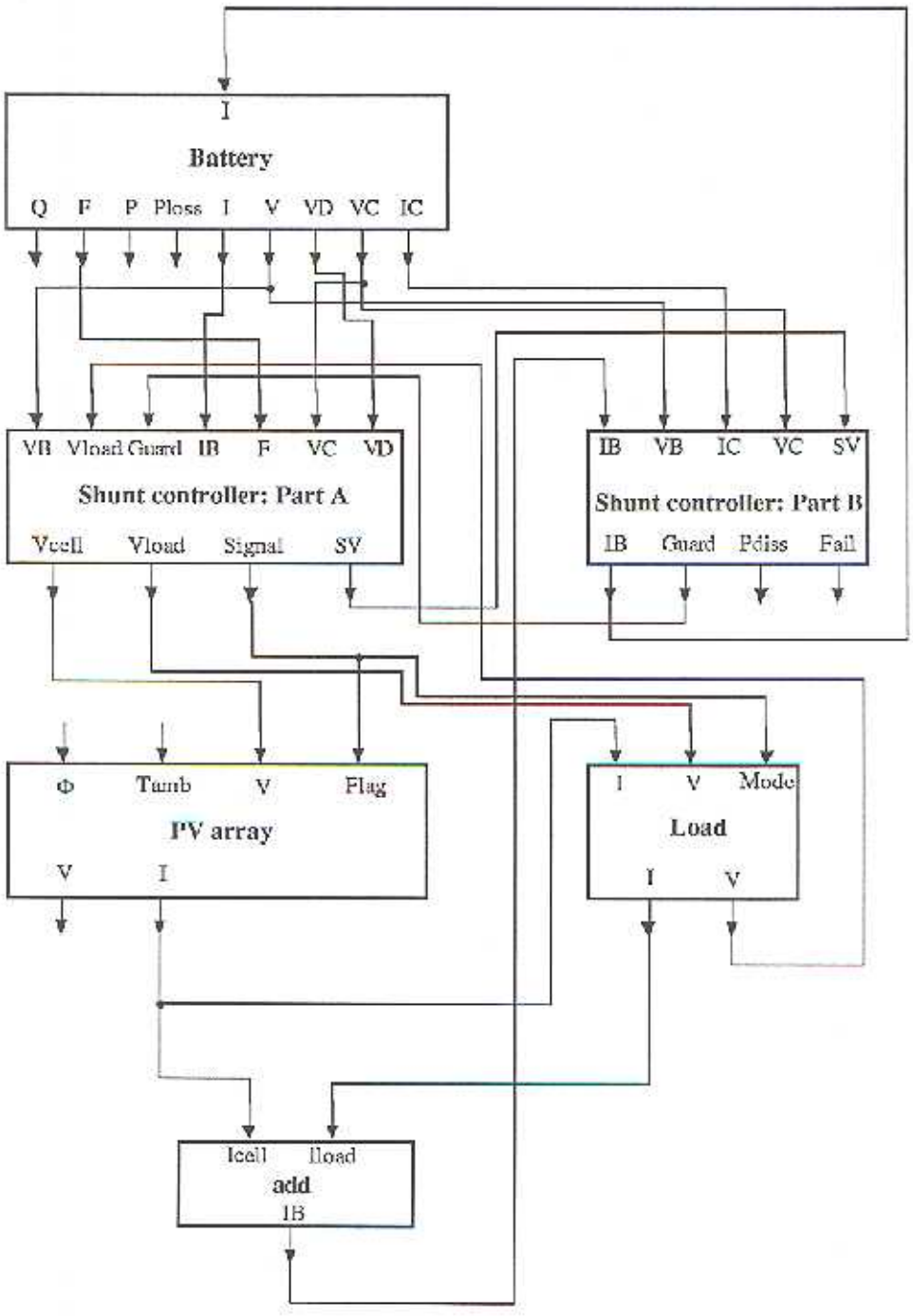

Figure 4.11 TRNSYS system configuration of a PV system including battery storage and a shunt type controller

Considering the normal operation mode (where the battery SOC and the battery terminal voltage are within the specified limits) the current goes into the battery and the resulting voltage is shifted to the controller part A. The voltage across the load has the same magnitude as the battery voltage. In this case, the switch of the undervoltage protection device is closed. The cell voltage differs from the battery voltage by the magnitude of the voltage drop of the diode according to equation (4.3.1).

The voltages are shifted to the PV array and the load component and generate the corresponding currents. These currents are transferred to the add device which determines the battery current corresponding to equation (4.3.2). At the normal operation code, the battery current is passed through the shunt controller part B and returned to the battery component. The process described is iterative. Starting with an initial guess, the iteration will continue until the convergence tolerance on all inputs is satisfied and thus the operating point is found.

The shunt controller part A performs the checks on F and the battery voltage. Assuming the battery is being charged and the battery voltage would exceed the upper limit on voltage or gassing voltage, V_C. In this case the controller will switch to a trickle charge mode. The voltage is reduced to V_C by limiting the battery current to the current corresponding to V_C, which is I_C. Physically this is done by shunting current through the overvoltage protection branch as explained above. In TRNSYS, this is done by sending a signal, SV (SV = 3), to the controller part B. Controller part B sets I_C which it takes from the battery equal to I_B and returns this reduced current back to the battery. It also evaluates the involved dissipated power which is

$$P_{diss} = (I_B - I_C)\, V_C \qquad (4.3.3)$$